Rational Design of Functional DNA with a Non-Ribose Acyclic Scaffold

Hiromu Kashida,[a] Xingguo Liang,[a] and Hiroyuki Asanuma[*,a,b]

[a]*Graduate School of Engineering, Nagoya University, Furo-cho, Chikusa-ku, Nagoya 464-8603, Japan*

[b]*Core Research for Evolution Science and Technology (CREST), Japan Science and Technology Agency (JST), Kawaguchi, Saitama 332-0012, Japan*

Abstract: The growing field of DNA technology requires new modified DNAs that can perform advanced functions. No matter how we optimize the length and sequence of DNA using only the four naturally occurring nucleotides, potential performance is limited. In this review, we describe a facile and effective method of rationally designing new functional DNA by focusing on acyclic scaffolds, especially threoninols, which are utilized to incorporate functional molecules into DNA. Wedge-type insertion of a functional molecule with a planar structure of proper size in D-threoninol to DNA does not destabilize the duplex, although the backbone structure is changed. Rather, intercalation offsets such distortions and significantly raises the melting temperature of the DNA duplex. Based on the wedge-type insertion, photoresponsive DNA (tethering azobenzenes) and fluorescent probes that can detect single nucleotide polymorphisms (SNPs) and insertion/deletion (indel) polymorphisms have been designed. Furthermore, a variety of molecular clusters of dyes have also been prepared from acyclic scaffolds tethering dyes.

1. INTRODUCTION

DNA, which is composed of four nucleobases, exhibits increasingly interesting and important functions in the fields of biochemistry, biotechnology, and nanomaterials due to its sequence specific recognition (hybridization) of the counter-strand and formation of a double-helical structure. The rule of hybridization is ingeniously simple: A only pairs with T, and G only with C. In early era of DNA research, only certain molecular biologists or synthetic organic chemists were able to create DNA. Starting in the 1980s, advances in chemical DNA synthesis resulted in DNA synthesizers becoming commonplace, which has enabled the commercial production of DNA at a reasonable cost. At present, we can obtain DNA of any sequence within a few days, as long as its length is not overly long, e.g., below 100 nucleotides. Such easy access to DNA has dramatically increased its use by researchers other than organic chemists and biologists. DNA technology has been spreading through various fields of science and technology, thus demonstrating its high potentiality: with DNA, we can perform computation [1], build nano-wires [2], construct and manipulate molecular machines [3], and even draw nano-pictures [4]. Presently, DNA (and also RNA) has become a key macromolecule not only for biochemistry or biotechnology but also material science.

However, the growing field of "DNA technology" requires new modified DNAs that can perform more superior functions. Unlike proteins or oligopeptides composed of as many as 20 amino acids, naturally occurring DNA has only four "silent" nucleobases. No matter how we optimize the length and sequence, the potential performance is limited as long as only these four nucleobases are used. Accordingly, necessary functions that cannot be achieved with these nucleobases must be supplied with non-natural molecules. This important requirement, coupled with progress in synthetic chemistry, has created a demand for new, rationally modified DNAs. As a result, various methods for placing functional molecules have been proposed, and numerous modified DNAs have been synthesized [5].

1.1. Modification of Natural Nucleosides

For the introduction of unnatural molecules into DNA, attention has to be paid to sequence specificity and the stability of the duplex. Except for tethering the molecule at the 5' or 3' termini, such as with fluorescent labeling, incorporation into the interior of DNA often changes the local structure (or the higher-order structure), which in some cases significantly lowers the intrinsic stability of the duplex and reduces sequence specificity. Hence, efforts should be made to minimize these drawbacks in order to maximize the performance of modified DNA. One solution to the above problem is the insertion of functional molecules into natural nucleotide units. The most popular modification points are the 5-position of thymine, 2'-position of ribose, and the phosphodiester linkage [6-10]. Since these modifications keep both hydrogen bonding between the nucleobases and the basic framework of the strand intact, structural perturbations are minimized. Modified DNAs with fluorescent molecules at these positions can be used as efficient probes that recognize SNPs and mRNA in a sequence-specific manner [11,12]. In particular, for modification at the 5-position, corresponding modified thymidine triphosphates can be incorporated into DNA by various DNA polymerases [13]. By utilizing these modified triphosphates, functional molecules that are incompatible with conventional solid-phase synthesis based on phosphoramidite chemistry are easily introduced into the oligonucleotide.

*Address correspondence to this author at the Graduate School of Engineering, Nagoya University, Furo-cho, Chikusa-ku, Nagoya 464-8603, Japan; E-mail: asanuma@mol.nagoya-u.ac.jp; Fax: +81-52-789-2528; Tel: +81-52-789-2488.

1385-2728/09 $55.00+.00

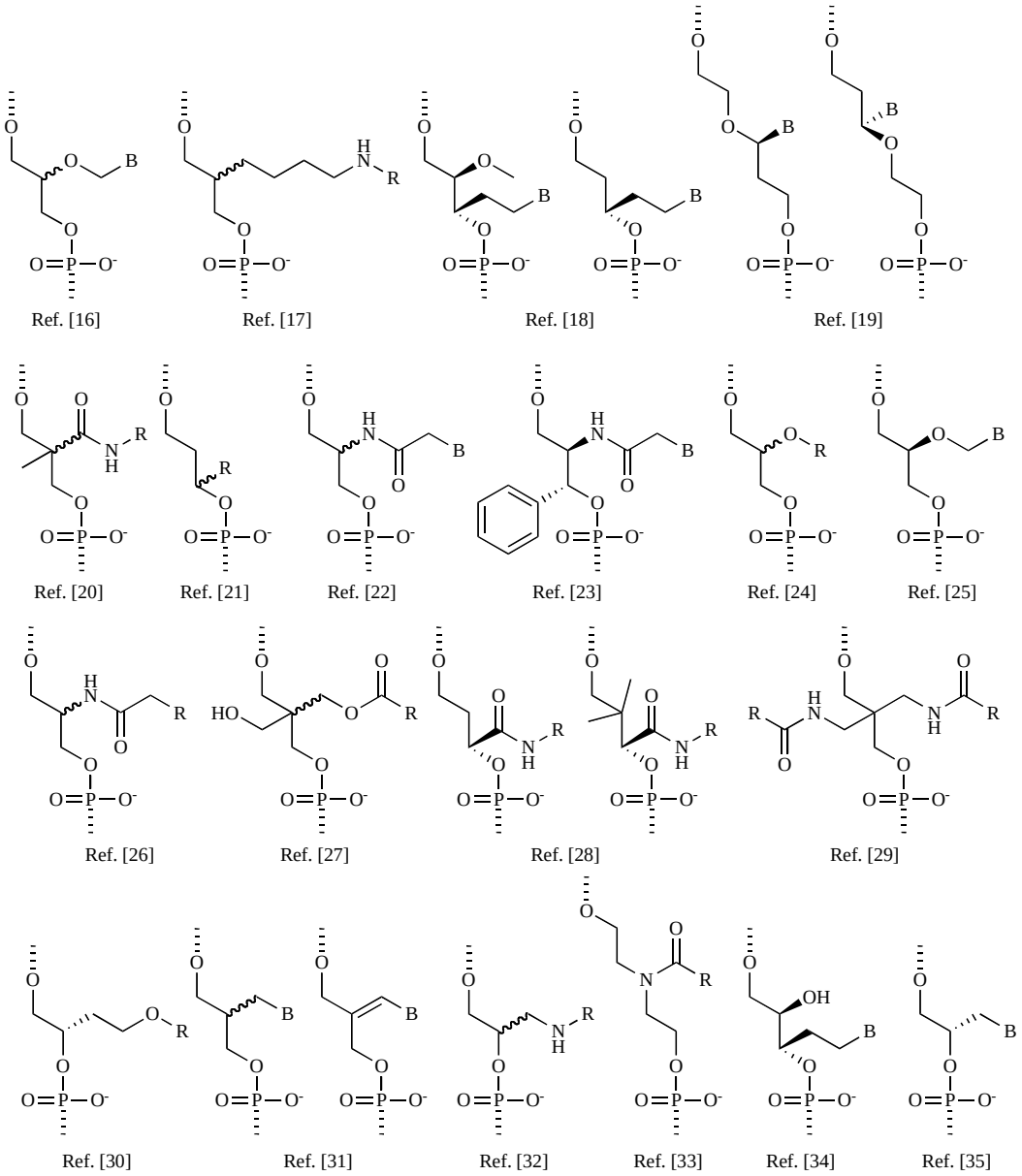

Fig. (1). Acyclic scaffolds for tethering natural nucleobases and non-natural molecules.

Although direct modification of natural nucleotide units has its advantages, there are several synthetic difficulties: all four (A, T, G, and C) corresponding modified phosphoramidite monomers have to be synthesized in order to apply them to various sequences. Modification of thymidine is relatively easy because the corresponding monomer does not need base protection, while for the other three nucleotides, the amino group on these bases should be protected. In fact, most modifications have been carried out only on thymidine to avoid such laborious protection processes. Modification of the phosphodiester linkage is also difficult from the viewpoint of stereoregulated synthesis: two diastereomers with respect to the chirality of the phosphorous atom are inevitably produced with conventional phosphoramidite chemistry without a special synthetic technique [14]. Furthermore, direct modification does not necessarily stabilize the duplex even when structural perturbation is minimized. In some cases, duplexes are significantly destabilized [15].

1.2. Merits of Utilizing Acyclic Scaffolds for Incorporating Functional Molecules as Base Surrogates

Compared to the direct modification of nucleotide units as discussed above, the utilization of acyclic diols as scaffolds is a more effective method. A functional molecule (or natural nucleobase) is tethered to the acyclic diol, which is incorporated into the DNA through the corresponding phosphoramidite monomer. As shown in Fig. (**1**), various acyclic scaffolds have been used to tether natural nucleobases and non-natural molecules [16-35]. Among these scaffolds, ethylene glycol (abbreviated as a C2 scaffold because there are two carbon atoms between the inter-phosphodiesters) and 1,3-propanediol (abbreviated as a C3 scaffold) derivatives are most frequently used due to their structural similarity to natural D-ribose (Fig. **2a**). This strategy has several advantages when tethering functional molecules other than nucleobases, although the scaffolds change the backbone structure of DNA to some extent:

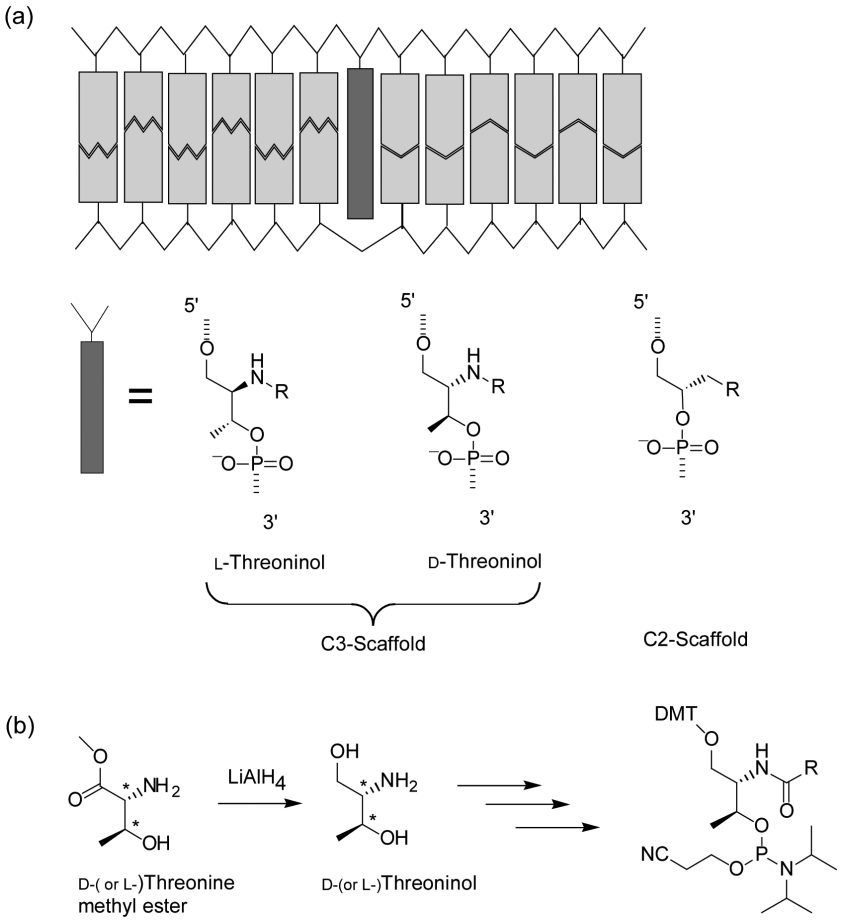

Fig. (2). Wedge-type (bulge-type) insertion of a functional molecule via C3- and C2-scaffolds (a) and conversion of a D-(or L-)threoninol derivative to phosphoramidite monomer (b).

1) A functional molecule on the scaffold can be introduced at any position in the sequence; we do not have to synthesize four corresponding monomers. Introducing different kinds of functional molecules to one strand of DNA at the desired positions is also possible.
2) Synthetic complexity is greatly reduced as compared with direct modification of nucleotide units. Starting from a reaction of flanking a functional molecule on a scaffold, only three steps are necessary to synthesize the corresponding phosphoramidite monomer.
3) Base surrogates with acyclic linkers allow a variety of sequence designs: wedge-type (bulge-type) insertion, nucleotide analog, or the pairing of the base surrogate with a natural nucleotide or the base surrogate itself.

One might think that the use of acyclic scaffold would change the backbone structure and lower the stability (melting temperature) of the DNA duplex drastically. However, incorporated functional molecules can compensate for instability, and in some cases, *overcompensate* for it. Since most functional molecules to be incorporated, such as dyes, take a planar structure, stacking interactions make the unstrained duplex tight.

In this review, we describe a facile but effective method of rationally designing functional DNA by focusing on acyclic scaffolds that are utilized to incorporate functional molecules, with particular focus on our recent works.

2. THREONINOL AS AN EFFECTIVE SCAFFOLD FOR THE WEDGE TYPE INSERTION

First, from the viewpoint of duplex stability, we describe a wedge-type (bulge-type) design on threoninol linker as depicted in Fig. (**2a**). Threoninol (2-amino-1,3-butanediol), which is easily obtained by one-step reduction of threonine methyl ester, is a very convenient C3 scaffold. A molecule attached to a carboxyl group is easily conjugated to the primary amine of threoninol through the amide bond and incorporated into DNA via the corresponding phosphoramidite precursor as illustrated in Fig. (**2b**). Unlike other C3 scaffolds such as serinol or glycerol, four optically pure threoninols with respect to the two chiral carbons are available. Furthermore, the methyl group on the threoninol facilitates conversion to a phosphoramidite monomer, because 4,4'-dimethoxytrityl chloride is selectively coupled with the primary hydroxyl group (see Fig. **2b**). Reynolds et al. first used L-threoninol as a scaffold to tether a psolaren for photocrosslinking of a target m-RNA [36]. Fukui *et al.* later conjugated acridine on L-threoninol and hybridized it to DNA to investigate the effect of the linker between the threoninol

Table 1. Effect of Configuration of the Scaffold on the Stability of the Duplex

Entry	Strand [a,b]	T_m/°C [c]		ΔT_m/°C [d]	Ref.
		trans	*cis*		
6-N	5'-CGAGTC-3'	30.1			[40]
6-W	5'-CGA**W**GTC-3'	25.5[e]			-
6-D	5'-CGA$\mathbf{Z_D}$GTC-3'	37.7	14.0	23.7	[40]
6-L	5'-CGA$\mathbf{Z_L}$GTC-3'	33.7	22.3	11.4	[40]
6-R	5'-CGA$\mathbf{Z_R}$GTC-3'	37.1	11.5	25.6	[40]
6-S	5'-CGA$\mathbf{Z_S}$GTC-3'	32.7	15.7	17.0	[40]
8-D	5'-GCGA$\mathbf{Z_D}$GTCG-3'	50.9	36.6	14.3	[39]
8-L	5'-GCGA$\mathbf{Z_L}$GTCG-3'	45.1	40.8	4.3	[39]
8-LL	5'-GC$\mathbf{Z_L}$GAGT$\mathbf{Z_L}$CG-3'	25.4	25.5	-0.1	[39]
8-DL	5'-GC$\mathbf{Z_D}$GAGT$\mathbf{Z_L}$CG-3'	31.9	22.2	9.7	[39]
8-LD	5'-GC$\mathbf{Z_L}$GAGT$\mathbf{Z_D}$CG-3'	38.7	22.9	15.8	[39]
8-DD	5'-GC$\mathbf{Z_D}$GAGT$\mathbf{Z_D}$CG-3'	43.9	22.4	21.5	[39]

a) 3'-GCTCAG-5' was used as a complementary counterpart of the 6-*n* series, whereas 3'-CGCTCAGC-5' was used for the 8-*n* series.
b) Structure of each surrogate is shown below.
c) Melting temperatures were measured at pH 7.0 (10 mM phosphate buffer) in the presence of 1.0 M NaCl. Conc. of each strand was 50 μM.
d) Change of *T*m induced by *trans*-*cis* isomerization.
e) Newly determined for this review.

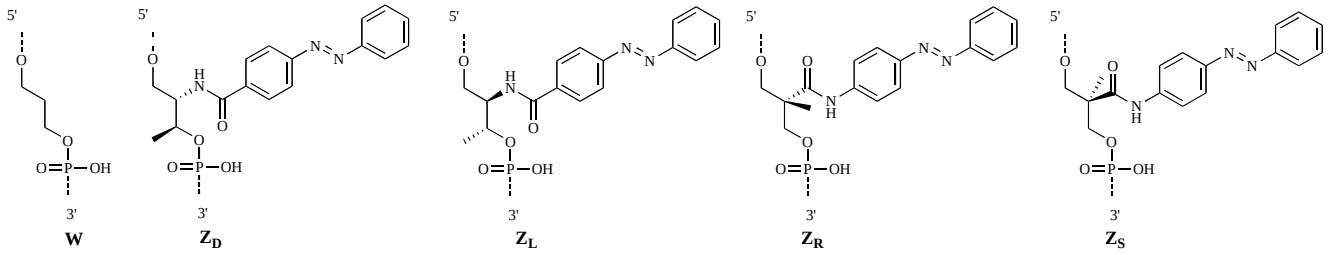

and acridine [37,38]. In both cases, these molecules were introduced into DNA as wedge-type insertions, and the sequence design stabilized the duplex due to the intercalation of these planar molecules. In contrast, the introduction of an acridine moiety opposite of a natural nucleotide to form an acridine-base mismatch pattern in the counterstrand destabilizes the duplex due to steric hindrance [38].

2.1. D-Threoninol as a Superb Scaffold for Functional Molecules

Although the feasibility of L-threoninol as a scaffold has been demonstrated, the effect of chirality on stability has not been discussed. Our group has used both D-threoninol and L-threoninol to tether azobenzene for the photoregulation of DNA function (*vide infra*), and found that D-threoninol is far superior to the L-form [39]. This chirality effect is primarily based on its winding property: D-threoninol prefers clockwise winding whereas the L-form prefers counterclockwise winding. Since naturally occurring DNA forms a right-handed duplex whose winding is clockwise, the introduction of azobenzene through D-threoninol tends to stabilize the duplex. Table **1** shows the effect of the chirality of threoninol on the stability of corresponding DNA duplexes. The melting temperature (T_m) of native duplex without an azobenzene moiety (**6-N** in Table **1**) is 30.1 °C [40]. The insertion of a 1,3-propanediol linker (**6-W**) significantly lowers duplex stability because of the distortion of the main chain. On the contrary, conjugation of a *trans*-azobenzene to L-threoninol (**6-L**) significantly raises the T_m to 33.7 °C, which is about 8 °C higher than that of **6-W**, and even higher than that of the native **6-N** duplex, demonstrating that intercalated planar *trans*-azobenzene *overcompensates* for the distortion caused by the insertion of the C3 scaffold [36-39]. Interestingly, azobenzene in D-threoninol stabilizes the duplex much more than its enantiomer L-threoninol: the T_m of **6-D** is as high as 37.7 °C [40]. Exactly the same tendency was observed for $\mathbf{Z_R}$ and $\mathbf{Z_S}$ that were synthesized as a mixture with a prochiral C3 scaffold (2,2-bis(hydroxymethyl) propionic acid) and separated by HPLC after incorporating them into DNA [41,42]. Scaffolds having the same configuration ($\mathbf{Z_D}$ and $\mathbf{Z_R}$, or $\mathbf{Z_L}$ and $\mathbf{Z_S}$) give almost the same T_m (compare **6-D** with **6-R**, and **6-L** with **6-S** in Table **1**), demonstrating that the proper orientation of the flanking intercalator is essential for stabilizing the duplex.

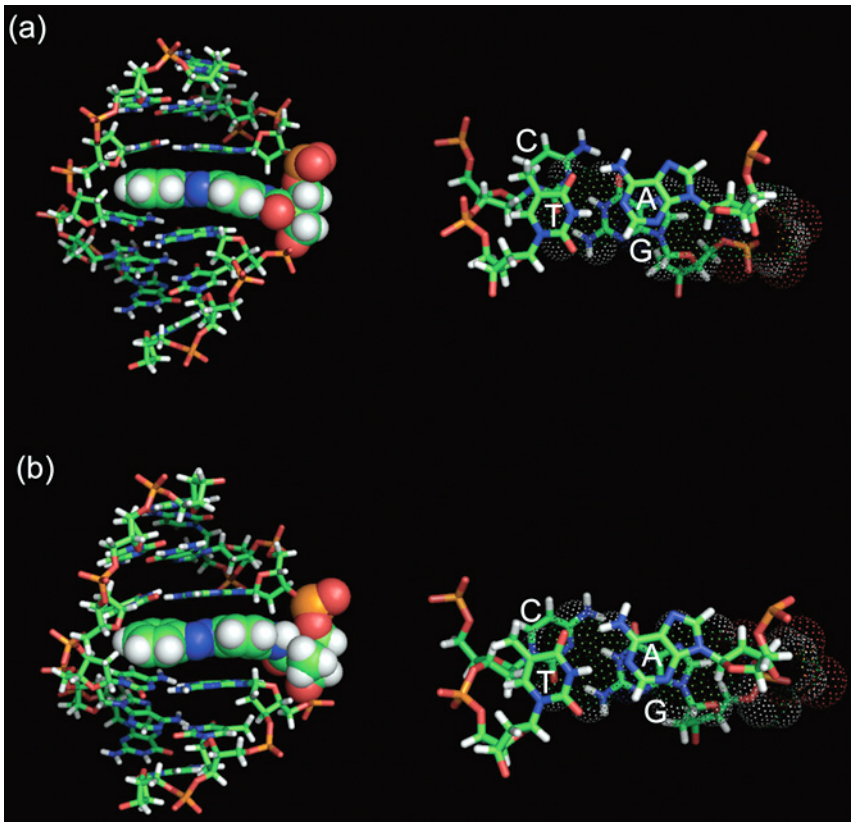

Fig. (3). Minimized average structures of 5'-C^{1}G^{2}A^3**X**G^{4}T^{5}C^6-3'/3'-G^{7}A^{8}C^{9}T^{10}C^{11}G^{12}-5' duplexes where **X** denotes (a) $\mathbf{Z_R}$ (corresponding $\mathbf{Z_D}$) and (b) $\mathbf{Z_S}$ (corresponding $\mathbf{Z_L}$) viewed from the side of azobenzene (left panel) and their stacked structures (right panel) around the **X** residue viewed from the 5'-side of the helix axis. For the top view (right panel), only the 5'-A^3**X**G^4-3'/3'-T^{10}C^9-5' part is depicted and azobenzene is drawn as a dot surface for clarity.

The winding property of the scaffold has been revealed by NMR analysis. Fig. (**3**) shows the solution structures of duplex 5'-CGA$\mathbf{Z_R}$GTC-3'/3'-GCTCAG-5' (**6-R** in Table **1**) and duplex 5'-CGA$\mathbf{Z_S}$GTC-3'/3'-GCTCAG-5' (**6-S**) determined from NOESY. Although the structures of both duplexes are very similar, a slight difference is observed around the azobenzene: the skew angle between A^3-T^{10} and G^4-C^9 for $\mathbf{Z_R}$ (corresponds to $\mathbf{Z_D}$) is 35-36° (right panel in Fig. **3a**), whereas that for $\mathbf{Z_S}$ (corresponds to $\mathbf{Z_L}$) is 30-31° (left panel in Fig. **3b**) [40]. Note that the B-type helix has about 10 base pairs per turn, and hence the skew angle of the natural duplex is 36°. Intercalation of the *trans*-azobenzene on D-threoninol does not disturb the right-hand helix. On the other hand, the skew angle for $\mathbf{Z_S}$ is 5-6° smaller than that for $\mathbf{Z_R}$, demonstrating that winding of the helix is slightly disturbed on L-threoninol. Accordingly, the melting temperatures for **6-D** and **6-R** are higher than those of **6-L** and **6-S** (Table **1**).

The difference in stabilization of the duplex between the two configurations is further amplified by introducing more insertions, e.g. introduction of two molecules greatly affects the T_m. As listed in Table **1**, the T_m of **8-LL** which tethers two azobenzenes on L-threoninols is as low as 25.4 °C, whereas that of **8-DD** with D-threoninol is about 20 °C higher (43.9 °C). Counterclockwise winding of L-threoninol does not greatly affect the stability when one surrogate is inserted, partly because the intercalation of azobenzene offsets the distortion. However, two (or more) intercalators on L-threoninols greatly disturb the original right-handed double helix, probably because the intercalators cannot assume the proper configurations for stacking. All of the above results support the conclusion that D-threoninol, which prefers clockwise winding, is an appropriate scaffold to tether functional molecules, especially for the introduction of multiple intercalators.

2.2. Requisites for Functional Molecules that Do Not Cause Destabilization of the Duplex

As described in the previous section, destabilization caused by the insertion of one threoninol is more than offset by *trans*-azobenzene, because its planar structure works as an efficient intercalator and thus stabilizes the duplex by stacking interactions. However, not all functional molecules stabilize the duplex. Non-planar *cis*-azobenzene significantly destabilizes the duplex due to steric hindrance between the intercalated *cis*-azobenzene and adjacent base-pairs (Table **1**) [39,40]. One important factor for stabilizing the duplex is the molecular size of the tethered functional molecule (Fig. **4**). Since the size of the Watson-Crick base-pair is around 11 Å [43]. Intercalated functional molecules of a similar size (9 – 11 Å) such as stilbazole and antraquinone reasonably fit the internal space between adjacent base-pairs and stabilize the duplex. However, *para*-substitution of the distant benzene

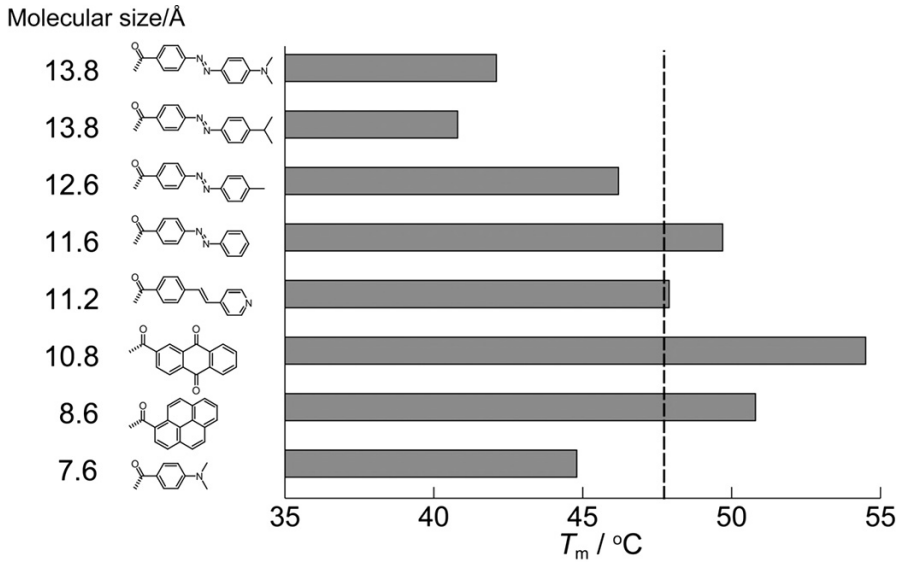

Fig. (4). Effect of molecular size of tethered functional molecules on D-threoninol (**X** residue) on the melting temperature of the duplex (5'-GGTATC**X**GCAATC-3'/3'-CCATAGCGTTAG-5'). The dashed line shows the melting temperature (47.7 °C) of the native duplex without the **X** residue.
Conditions: [DNA] = 5 μM, [NaCl] = 100 mM, pH 7.0 (10 mM phosphate buffer).

ring of azobenzene (Methyl Red, *p*-methyazobenzene, and *p*-isopropylazobenzene) significantly lower the T_m because these molecules are too long to intercalate due to steric hindrance between the substituted groups and the backbone of the complementary strand. Destabilization also occurs when a smaller sized intercalator, such as aniline, is tethered to threoninol because of insufficient stacking interactions, which is similar to introducing a bulge nucleotide. Thus, for improving stability of the duplex, we can modify the structure and change the molecular size of the functional molecule.

2.3. Comparison of D-threoninol with Deoxyribose as a Scaffold for Wedge-Type Insertions

Wedge-type insertions are also possible with a traditional deoxyribose scaffold, to which a non-natural molecule is tethered. Leumann *et al.* tried such an insertion of a pair of bipyridyl or biphenyl groups on both strands of a DNA duplex. Although the molecular size of the introduced non-natural molecule is 9.7 Å, which is much larger than that of the nucleotide base, the T_m of the duplex was almost the same as that without the insertions [44]. Ohuchi *et al.* described the thermodynamic parameters of a single-bulge insertion (wedge-type insertion) based on a pseudo-nearest neighbor model (5'-NNN-3'/3'-NN-5'). Irrespective of the sequence, the ΔGs of all the combinations were positive, indicating that a single-bulge destabilized the duplex [45]. In contrast, the ΔGs of 5'-N**Z**$_{\mathbf{D}}$N-3'/3'-NN-5' in which an azobenzene was tethered on D-threoninol were negative irrespective of the neighboring bases [46]. In other words, in any sequence, the wedge-type insertion of azobenzene via D-threoninol stabilizes the duplex. Although we cannot fairly evaluate the stabilizing effects of deoxyribose and D-threoninol scaffolds because their incorporated molecules are different, acyclic threoninol seems to be as good or better than deoxyribose for wedge-type insertions.

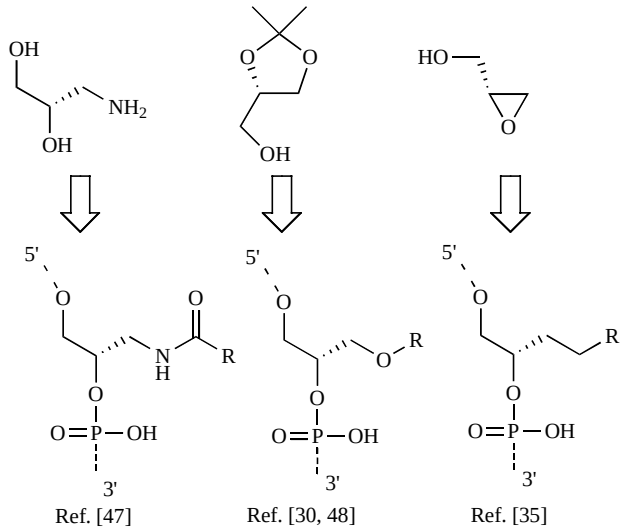

Fig. (5). Chiral starting materials for C2 scaffolds.

3. C2 SCAFFOLDS FOR THE WEDGE-TYPE INSERTION

In addition to threoninol, ethylene glycol derivatives involving two carbons in the main chain are also a promising candidate as a scaffold of wedge-type insertions. Either optically pure 3-amino-1,2-propanediol or 2,2-dimethyl-1,3-dioxolane-4-methaonol are conventionally available as starting materials, and functional molecules can be incorporated through ether bonds or amide bonds (see Fig. **5**) [30,35,47,48]. Chiral glycidol is also available for synthesizing C-nucleotide analogs [35]. Similar to threoninol, chirality also affects the duplex stability. Two optically pure glycerol derivatives were used as a starting material to tether pyrene, and the effect of chirality on the duplex was investi-

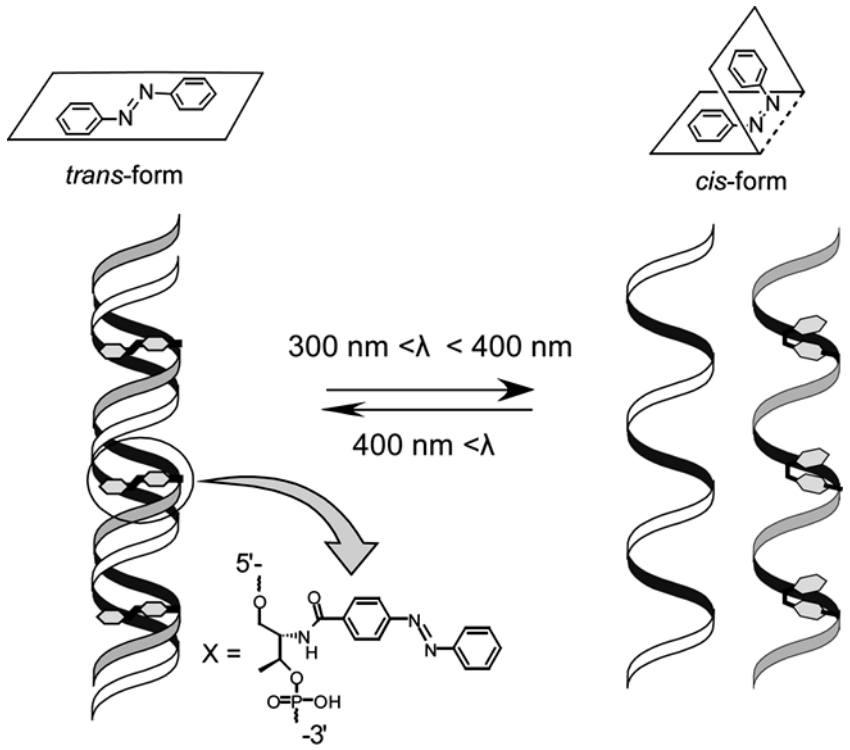

Fig. (6). Illustration of the photoregulation of DNA hybridization by photoresponsive DNA tethering azobenzenes on threoninol scaffolds.

Table 2. Effect of Chirality of the C2 Scaffold on Melting Temperature[a)]

Sequence	Melting Temperature / °C [b)]	
	X = 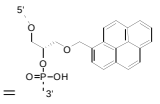	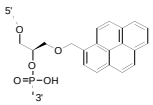
5'-CTCAAGCAAGCT-3'	48.0	
5'-CTCAAG**X**CAAGCT-3'	52.5	49.3

a) Data from Ref. [48]
b) Target DNA: 5'-AGCTTGCTTGAG-3', [DNA] = 1 μM in 140 mM NaCl, 10 mM phosphate buffer, 1 mM EDTA, pH 7.0

gated. As can be seen in Table **2**, the *S*-form stabilized the duplex more efficiently than the *R*-form did when the target was DNA [48]. This tendency is the same as observed for threoninol with a three-carbon backbone. An *S*-formed glycerol scaffold corresponding to D-threoninol showed a better stabilizing effect, indicating that the winding property is important for efficient stabilization in both C2 and C3 scaffolds. With this C2 scaffold, multiple introductions of pyrene into DNA are possible without destabilizing the duplex [48].

4. PHOTOREGULATION OF DNA FUNCTION WITH AZOBENZENE-TETHERED DNA ON A THREONINOL SCAFFOLD

In previous sections, we discussed the potential of acyclic scaffolds due to their duplex stability. By use of these scaffolds, various functional molecules are easily incorporated into DNA at any position and in any number without significant loss of stability and sequence specificity. These excellent properties are promising for various applications. In the following sections, several applications that have already been achieved are described.

The first example is the design of photoresponsive DNA for photoregulating DNA function, which has recently aroused much interest. Photoregulation of a biologically active compound related to DNA can be used as a robust tool for investigating particular biological phenomena and mechanisms in living cells, which may otherwise be very difficult to achieve [49-53]. As an external stimulus, photocontrol has the following advantages: 1) light does not contaminate the reaction system, 2) the excitation wavelength is controllable by designing the photoresponsive molecule, and 3) control of irradiation time and/or local excitation is easy. For this purpose, the introduction of photo-isomerizable azobenzene is one effective way to provide photoresponsiveness to DNA [54-56]. We discuss below an example using threoninol as a scaffold to incorporate azobenzene.

4.1. Photoregulation of Hybridization with Azobenzene on D-threoninol

Spontaneous hybridization of DNA (or RNA) with its complementary counterstrand is a fundamental supramolecular property that is involved in most nucleic acid-specific enzymatic reactions. Hence, if double-stranded DNA can be converted into two single-strands reversibly by photoirradiation at a predetermined place and at a desired time, as illustrated in Fig. (**6**), a variety of useful applications are possible. For this purpose, azobenzenes were introduced into DNA with threoninol as a scaffold. As shown in Table **1**,

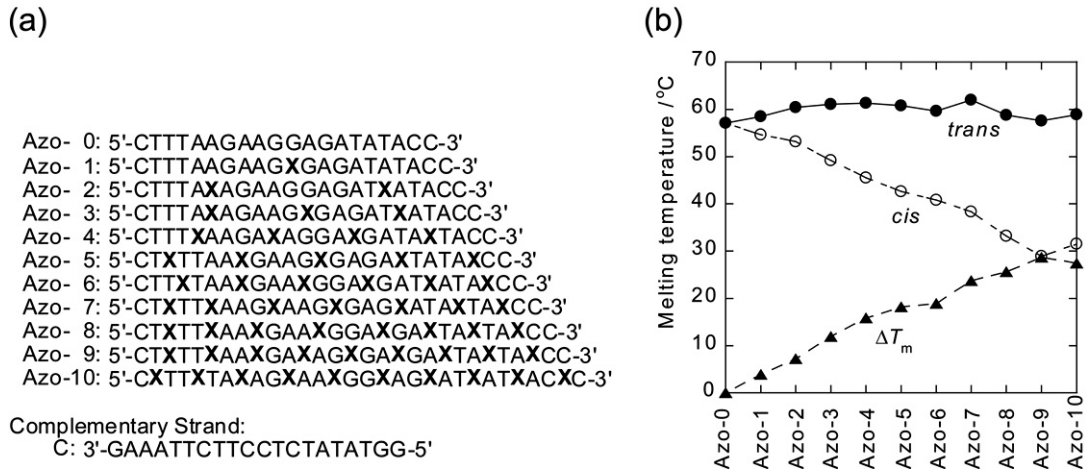

Fig. (7). Incorporation of multiple azobenzenes on D-threoninol (**a**) and effect of the number of azobenzenes on melting temperature at pH 8.0 (10 mM Tris-HCl buffer) in the presence of 10 mM $MgCl_2$, 50 mM NaCl.

trans-azobenzene (visible light irradiation) stabilizes the duplex by stacking interactions whereas *cis*-azobenzene (UV light irradiation) greatly destabilizes it by steric hindrance [39,42]. For this mode of photo-switching, D-threoninol is much more favorable than its enantiomer as a scaffold because it enhances the change of T_m (ΔT_m) induced by *trans-cis* isomerization, as shown in Table **1**. The superiority of D-threoninol becomes evident when multiple azobenzenes are introduced: the ΔT_m of **8-LL** tethering two azobenzenes on L-threoninols is –0.1 °C, whereas that of **8-DD** on D-threoninols is as large as 21.5 °C. Improvement of ΔT_m is also attained by modification at the *ortho* position of the distant benzene ring of azobenzene [57]. By multiplying azobenzenes on D-threoninols, even 20-nt-long DNA can be efficiently photoregulated.

As shown by closed circles in Fig. (**7b**) [46] the introduction of multiple azobenzenes does not interfere with duplex formation at all when they take the *trans*-form; the T_m of **Azo-10/C** involving 10 azobenzenes with respect to 20-nt long DNA is 58.6 °C, which is even higher than that of natural **Azo-0/C** (57.1 °C). Such incorporation of multiple intercalators without the loss of duplex stability is possible only when D-threoninol is used as a scaffold. In contrast, T_m uniformly decreases with the number of azobenzenes when they take the *cis*-form (open circles in Fig. **7b**) and the minimum T_m (28.9 °C) is observed for **Azo-9/C**. The change of T_m induced by *trans-cis* isomerization for the **Azo-9/C** duplex is as great as 28.9 °C. Actual melting curves of the **Azo-9/C** duplex both in the *trans*- and *cis*-forms are depicted in Fig. 8a. Attachment of a fluorescence molecule (e.g. (6-fluorescein-6-carboxamido)hexanoate; FAM) and a fluorescence quencher (e.g. 4-(4-dimethylaminophenylazo)benzoic acid; Dabcyl) to the termini of **C** and **Azo-9**, respectively, allows quantitative evaluation of hybridization at a constant temperature [58]. When irradiated with visible light, azobenzene takes the *trans*-form and thus fluorescence from FAM is completely quenched by Dabcyl bound to the complementary strand at 37 °C due to duplex formation (closed circles in Fig. **8b**). Upon UV irradiation of this sample at 37 °C, azobenzene is isomerized to the *cis*-form so that fluorescence from FAM recovers. As evaluated from the recovery of fluorescence intensity, 50% of the FAM-DNA dissociates while the other half remains hybridized with Dabcyl-DNA (triangles in Fig. **8b**). Upon UV irradiation to this sample solution at 60 °C followed by cooling to 37 °C, the recovered fluorescence from FAM-DNA is much larger than that with irradiation at 37 °C (open circles in Fig. **8b**), demonstrating that 85% of the FAM-DNA dissociates from Dabcyl-DNA [58]. In this way, photoregulation of hybridization is directly evidenced by the fluorophore-quencher system. These processes are totally reversible so that formation and dissociation of the duplex can be repeated by irradiation with UV or visible light without deterioration (see Fig. **8b**).

As shown in Fig. (**8b**), photoregulatory efficiency depends on the temperature of UV irradiation. In the single-stranded state, 60-70% of total azobenzene in photoresponsive DNA is easily isomerized to the *cis*-form irrespective of the UV-irradiation temperature. However, in the presence of its complementary strand, *trans*→*cis* isomerization is hindered at a temperature far lower than the T_m of the *trans*-form. Hence, 50% of the total DNA dissociates when UV irradiation is applied at 37 °C (note that the T_m of the ***trans*-Azo-9/C** duplex is 57.8 °C). In contrast, *cis*→*trans* isomerization by visible light irradiation occurs efficiently at any temperature, especially when the duplex is formed.

In addition to the duplex, triplex formation can be efficiently photoregulated by introducing azobenzene on an acyclic scaffold to a triplex-forming strand (TFO) [59-61]. In this case, the same strategy is applied to the TFO: azobenzene is tethered to oligothymidine on an acyclic linker such as 5'-**X**T_{13}-3', 5'-T_6**X**T_7-3', or 5'-**X**T_6**X**T_7-3' (**X** denotes the azobenzene moiety). A large ΔT_m between *trans*- and *cis*-forms is observed, indicating that the binding and release of these photoresponsive TFOs from the target duplex is efficiently photoregulated. Phenylazonatphthalene, in which the distant benzene ring of azobenzene is replaced with a larger naphthalene ring, also greatly improves the ΔT_m due to the eminent stabilization of the triplex in the *trans*-form [62]. Similar stabilization of triplexes is also observed for modified TFO tethering pyrene derivatives on a C2 scaffold, which can bind to the target duplex containing a GC base-pair at pH 7.2. This is a good example of utilizing acyclic

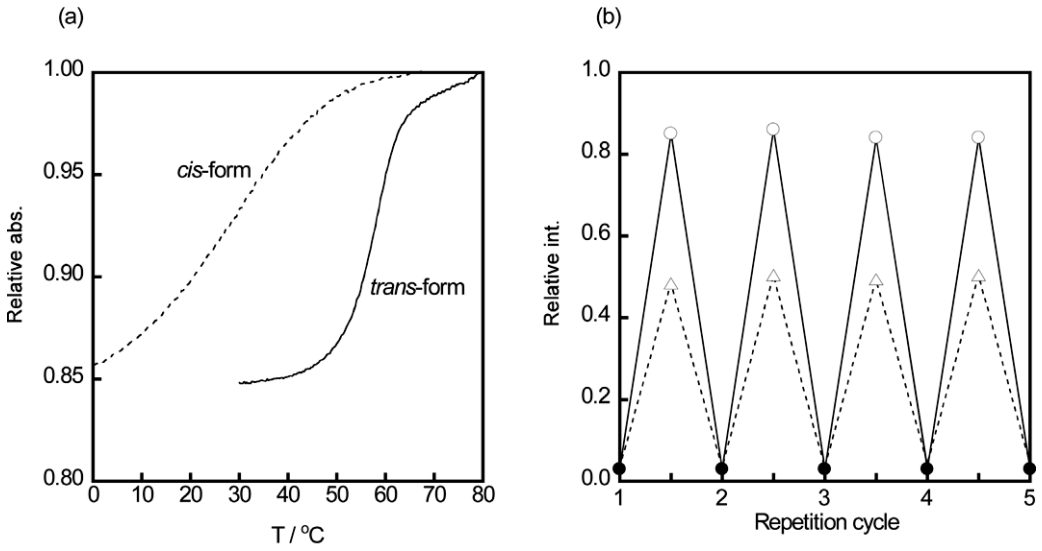

Fig. (8). Melting curves of the **Azo-9/C** duplex of *trans*-form (solid line) and *cis*-form (a), and its repeated hybridization (closed circles) and dehybridization (open circles or triangles) at 37 °C by UV and visible-light irradiation (b). [46,58]. The sequences of **Azo-9** and **C** are referred to in Fig. **7a**. The vertical axis of Fig. **8b** is the relative intensity of fluorescence from FAM-labeled **C** and Dabcyl-labeled **Azo-9** duplex with respect to that from FAM-**C** alone. Open circles denote UV irradiation at 60 °C whereas triangles denote that at 37 °C. Visible-light irradiation was conducted at 37 °C.
Conditions: [DNA] = 5 μM, pH 8.0 (10 mM Tris-HCl buffer) in the presence of 10 mM $MgCl_2$, 50 mM NaCl.

scaffolds because the native oligonucleotide involving cytidine can hardly bind to the same duplex target under the same conditions [63]. Since triple-helix formation is one of the most promising methods for sequence-specific recognition of DNA duplexes, these TFOs are promising for use in gene regulation based on an 'antigene strategy' that interferes with gene expression at both the transcription and translation levels [64].

4.2. Reversed Switching Mode of Hybridization with L-threoninol [65]

In the previous section, we described how *normal* photoswitching of DNA hybridization is achieved: *trans*-azobenzene turns on hybridization whereas the *cis*-form turns it off. Via molecular design of azobenzene and the scaffold, the photoswitching mode can be entirely reversed: *cis*-azobenzene turns *on* hybridization and the *trans*-form turns it off [65]. For this purpose, L-threoninol is now available. To achieve reversed photoregulation of hybridization, the duplex should be destabilized by *trans*-azobenzene as largely as possible, and destabilization by *cis*-isomerization should be minimized. As demonstrated in Fig. (**4**), an intercalator whose molecular size is larger than 12 Å destabilizes the duplex. Hence, a bulky group, such as isopropyl or *tert*-butyl, is attached at the *para*-position of azobenzene to enlarge steric hindrance with the DNA backbone to destabilize the duplex in the *trans*-form. In order to minimize the destabilization of *cis*-azobenzene, L-threoninol is used as the linker instead of D-threoninol. As described in section **4.1**, D-threoninol has been shown to be favorable for *normal* photoswitching because it facilitates the hybridization of modified DNA involving *trans*-azobenzene and largely destabilizes the duplex involving the *cis*-form. In the case of the L-form, the tethered azobenzene moiety stabilizes the duplex less in the *trans*-form, and the destabilizing effect of the *cis*-form is suppressed (see Table **1**), demonstrating that L-threoninol is useful for reversed photoswitching.

As designed, a combination of *tert*-butyl-modification at the *para*-position and L-threoninol entirely reverses the photoswitching mode. The ΔT_m of a normal photoswitch with unmodified azobenzene on D-threoninol (**Azo-D**) is +5.7 °C (Fig. **9a**). In contrast, when L-threoninol is used for tethering *tert*-butyl-modified azobenzene (**Azo-L**), the T_m of the *cis*-form far exceeds that of the *trans*-form: the T_m of the *trans*-form is as small as 38.6 °C, which is much lower than that of the *cis*-form (Fig. **9b**). As a result, ΔT_m becomes as *large* as -7.3 °C. This remarkable reversion of T_m is mainly attributed to the increase of T_m in the *cis*-form; the T_m of the *cis*-form (45.9 °C) is close to that of the native duplex (47.7 °C), indicating that the destabilization effect of the non-planar *cis*-structure is mostly offset by the stabilization effect of introduced *tert*-butyl group. In addition, such reversed photoswitching greatly improves the thermal stability of *cis*-azobenzene in the duplex state. At 25 °C, for example, the half-life of *cis*-**Azo-L** is 495 h in the presence of its complementary strand, which is about five times longer than that of its single-strand ($t_{1/2}$= 102 h). For the *normal cis*-**Azo-D** switch in the duplex, however, its half-life is not much different compared with that of the single-stranded state. The groove binding of *tert*-butyl in the case of *cis*-**Azo-L** suppresses the thermal *cis*→*trans* isomerization. Furthermore, *trans*→*cis* photoisomerization, which is suppressed in the *normal* **Azo-D** photoswitch in the duplex state, is also greatly improved with this *reversed* photoswitch, probably because of insufficient stacking of *trans*-azobenzene with adjacent base-pairs by steric hindrance of the *tert*-butyl group.

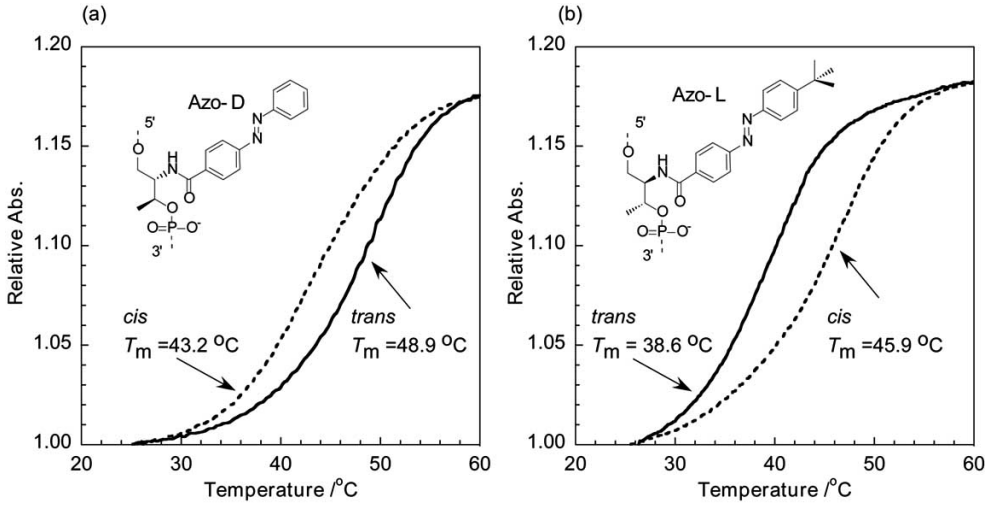

Fig. (9). Melting curves of 5'-GGTATC**X**GCAATC-3'/3'-CCATAGCGTTAG-5' duplex involving (a) **Azo-D**, (b) **Azo-L** residues at the **X** position for the *trans*-form (solid lines) and *cis*-form (dotted lines) by monitoring the change of absorbance at 260 nm. The temperature ramp was 1.0 ˚C/min. [NaCl] = 100 mM, pH 7.0 (10 mM phosphate buffer), [**DNA**] = 5 μM.

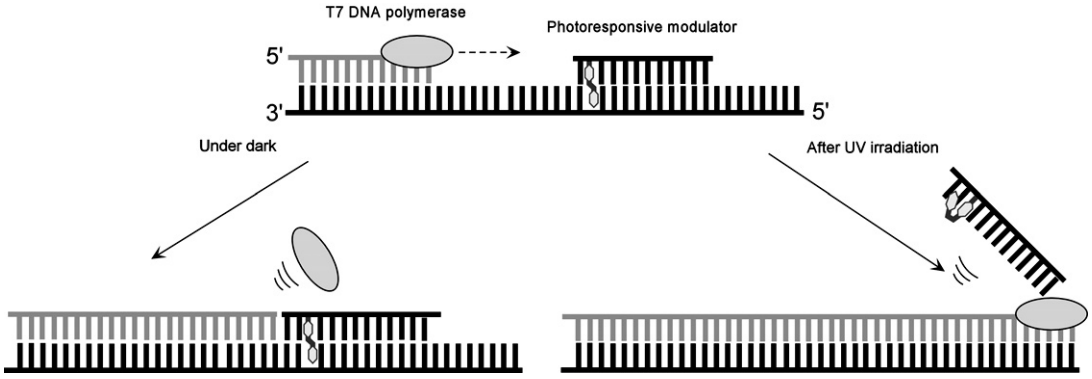

Fig. (10). Strategy for photoregulation of primer extension by T7 DNA polymerase with a photoresponsive modulator. Under dark conditions, the *trans*-modulator firmly hybridizes with the template and elongation stops before the modulator. After UV irradiation, however, the *cis*-modulator peels off from the template and elongation proceeds to the 5'-end of the template.

4.3. Photoregulation of Primer Extension by DNA Polymerase [66]

Since hybridization, the most fundamental property of DNA, can be photoregulated with azobenzene-tethered DNA, a wide variety of applications are possible. One example is the photoregulation of primer extension by DNA polymerase. The strategy is shown in Fig. (**10**). DNA of a predetermined length can be produced from one template by using photoresponsive DNA as a modulator with irradiating light of the appropriate wavelength. Azobenzene is tethered to the modulator whose 3'-terminus is protected by a 3-hydroxypropyl residue to avoid unexpected DNA elongation. When extension of a primer by T7 DNA polymerase that lacks 5'→3' exonuclease activity is conducted in the dark in the presence of the modulator, a short DNA is produced because DNA elongation is blocked by the modulator of the *trans*-form and stops at its 5'-terminus. Under irradiation of UV-light ($300 < \lambda < 400$ nm), however, the modulator of the *cis*-form can be peeled off and full-length DNA is predominantly produced [66]. Depending on whether there is light irradiation or not, either of these two DNAs can be selectively obtained from one template.

4.4. Photoregulation of RNase Reaction [67]

RNase H is known to hydrolyze RNA only when it hybridizes with its complementary DNA. Since this enzyme is closely related to the antisense effect in the cell [68], photoregulation of the RNase H reaction leads to the photoregulation of gene-expression based on the antisense strategy. This strategy is schematically illustrated in Fig. (**11a**) [67]. The initial solution contains substrate RNA, native antisense DNA without azobenzene, and corresponding sense DNA involving azobenzene moieties. The photoresponsive sense DNA in the *trans*-form strongly hybridizes with antisense DNA and thus the target RNA remains in the single-stranded state (upper panel in Fig. **11a**). Therefore, RNase H cannot digest RNA. Upon UV light irradiation, azobenzene moieties are isomerized to the *cis*-form and so antisense DNA is released. The released antisense DNA hybridizes with the target RNA, which is then hydrolyzed by RNase H (lower

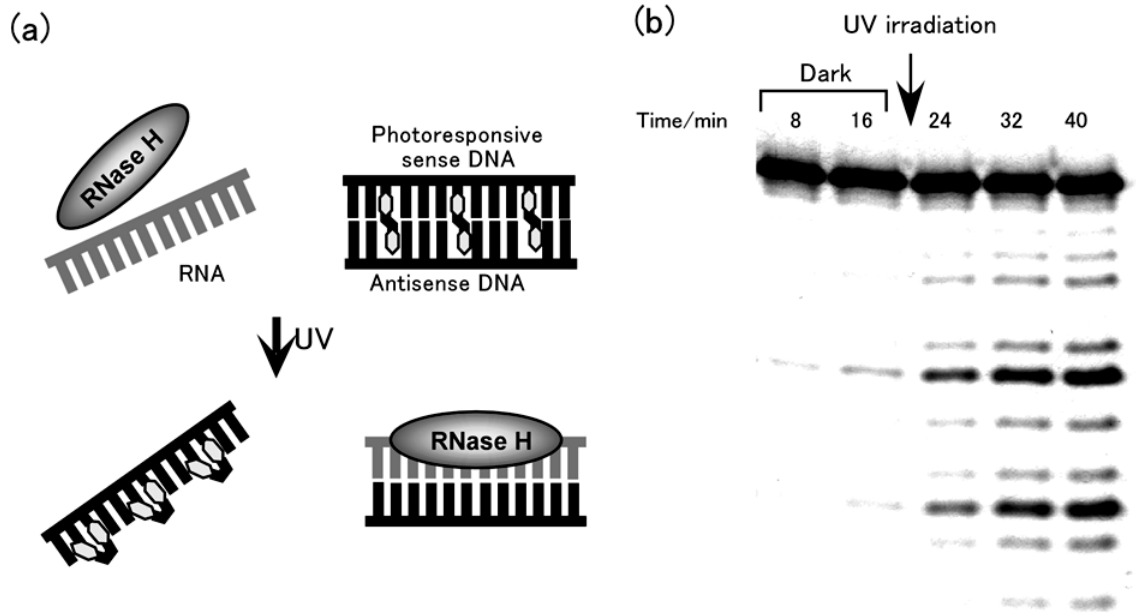

Fig. (11). Strategy for photoregulation of RNase H reaction (**a**) and time-course of UV light triggered RNA digestion by PAGE analysis (**b**). UV light was applied for 5 min after 16 min of incubation (at the arrowed position in Fig. **1b**) through a UV-D36C filter (from Asahi Technoglass). The intensity of UV light was below 100 μW cm^{-2}. Sequences of the DNA and RNA used here are listed below.

Photoresponsive sense DNA: 5'-CTTTA**X**AGAAG**X**GAGAT**X**ATACC-3
Antisense DNA: 5'-GGTATATCTCCTTCTTAAAG-3'
RNA: 5'-UAAGAAGGAGAUAUA-3'

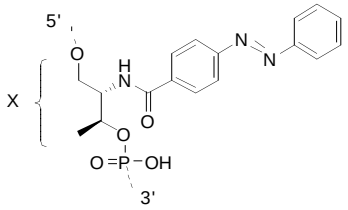

panel in Fig. **11a**). Although slight background scission by RNase H occurs, RNA digestion is fairly suppressed when azobenzene-tethered DNA hybridizes with antisense DNA in the reaction mixture under dark conditions (see lanes 1 and 2 in Fig. **11b**). Upon UV light irradiation, however, RNA is efficiently digested as expected (see lanes 3-5 in Fig. **11b**). Thus, off-to-on switching of RNA digestion by UV light irradiation can be attained. The photoregulatory efficiency of RNA digestion depends on the number of azobenzene moieties introduced into the sense DNA. As the number of azobenzenes in the sense DNA increases, photoregulatory efficiency is raised due to the enhancement of ΔT_m induced by *trans-cis* isomerization [67].

4.5. DNA Nanomachines Powered by Light-Irradiation

Photoresponsive DNA is applicable not only to enzymatic reactions as demonstrated above, but also to DNA nanotechnology, which proposes to employ DNA as a nanomaterial for constructing 2D- or 3D-nanostructures, or for DNA-based nanomachines [69-75]. Most DNA nanomachines generally use oligonucleotides as fuel. Mechanical motion is usually attained by the hybridization of one DNA strand to target sequences followed by removal with another strand that is completely or partially complementary to the first one [70] Yurke *et al.* first demonstrated a DNA machine that operates as "tweezers" fueled by two strands of DNA with tailored complementarity, as shown in Fig. (**12a**) [76]. Since the energy for operating these DNA nanomachines is produced by a strand exchange reaction, a duplex DNA is produced as a waste product in every working cycle. The accumulation of such "waste" duplexes gradually lowers the operating efficiency. In contrast, azobenzene-tethered DNA can hybridize and dehybridize with its complementary strand with only photoirradiation, leaving no waste in the reaction mixture. Hence, the use of photoresponsive DNA for a DNA nanomachine enables mechanical motion powered by light irradiation without producing any wastes during operation. Such 'environment-friendly' photon-fueled DNA tweezers can be constructed with azobenzene-tethered DNA with acyclic threoninols [77].

Photoresponsive DNA nano-tweezers composed of three strands (**A**, **B**, and **C**) have been designed as illustrated in Fig. (**12b**). The principle is simple: hybridization of strand **F** with single-stranded parts in the two arms (in strand **B** and **C**) closes the tweezers, whereas dissociation of **F** from **B** and **C** opens them. Azobenzene moieties are introduced into strand **F** so that the opening and closing of the tweezers can be photo-controlled by photoregulating the hybridization of strand **F** with **B** and **C**. As the *trans*-azobenzenes stabilize the duplex, the tweezers are closed after the solution is irradiated with visible light (440-460 nm); when the solution is irradiated with UV light (330-350 nm), however, the duplex

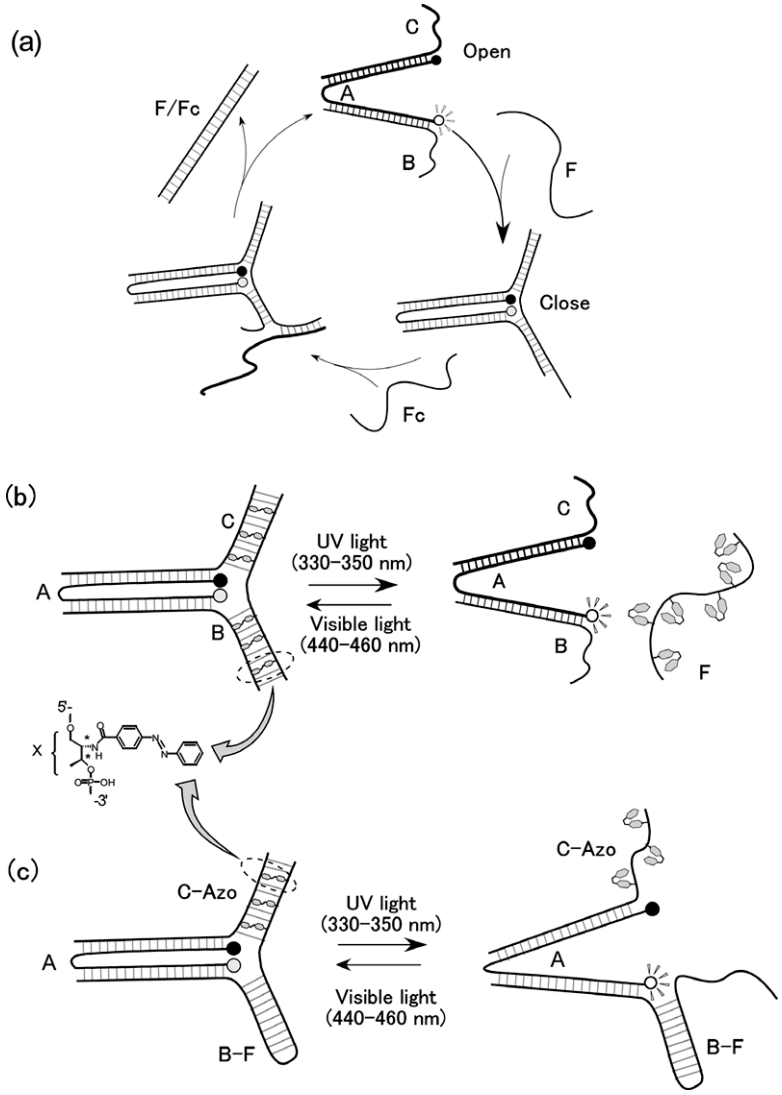

Fig. (12). Schematic illustration of working principles of DNA nano-tweezers. (**a**) Original tweezers constructed by Yurke *et al.* (**b**) Photoresponsive tweezers involving non-substituted azobenzenes tethered on D-threoninol. (**c**) Integrated photoresponsive tweezers by incorporating azobenzenes into the C strand (C-Azo) as an "engine".

dissociates due to the destabilization effect of *cis*-azobenzenes and the tweezers are open. At the 5′-end of **A**, a fluorophore (tetrachlorofluorescein, **TET**) is attached. The fluorescence emission of **TET** at around 540 nm (excited at 514.5 nm) can be quenched by resonant intramolecular energy transfer to **TAMRA** (carboxytetramethylrhodamine, a dye whose absorption band overlaps the emission band of **TET**) tethered at the 3′-end of strand **A**. As the efficiency of the resonant energy transfer increases with the decrease of distance between the two dyes, the opening and closing of the tweezers can be quantitatively monitored by measuring the fluorescence change of **TET**. Visible light irradiation (440~460 nm) of the solution involving **A**, **B**, **C,** and **F** at 50 ^{o}C for 1 min isomerizes the azobenzenes to the *trans*-form and the fluorescence from **TET** decreases due to the closing of the tweezers. On the other hand, UV light irradiation (330~350 nm) for 4 min at 50 ^{o}C isomerizes the *trans* to *cis*-form to open the tweezers and the fluorescence is recovered. The repeated opening and closing of photoresponsive DNA tweezers by successive light irradiation can be conducted without decreasing the efficiency after ten cycles, which is better than the original DNA-fueled tweezers: their cycling efficiency decreases by 40% after 7 cycles due to the successive addition of DNA fuel with the same sequences. Once the photoresponsive tweezers are constructed, the concentrations of all the oligonucleotides remain stable during the operation because no extra DNA oligonucleotides are added. Therefore, the photoregulatory efficiency does not change with additional operation cycles as long as the DNAs involved are not destroyed [77].

Original DNA-fueled tweezers are composed of a separate fuel strand and tweezers body, because the fuel has to be removed from the tweezers body to open them. With photoresponsive DNA, however, the fuel strand and the tweezers body are not necessarily separated. For example, by introducing azobenzenes into the **C** strand (**C-Azo** in Fig. **12c**)

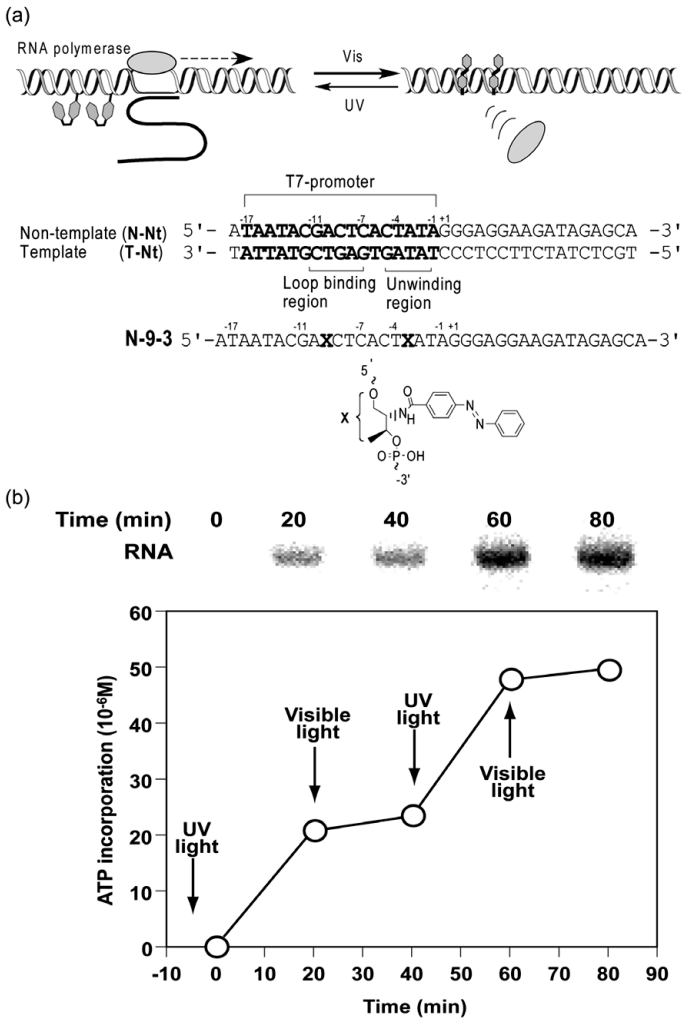

Fig. (13). Strategy for photoregulation of transcription by T7-RNA polymerase with photoresponsive T7-promoter (a), and light-switching of transcription by irradiation with UV light and visible light alternately with **N-9-3/T-Nt** at 37 ^{o}C (b). PAGE patterns (upper panel), and quantitative plots (lower panel) are depicted in (b). UV and visible light irradiation was carried out for 1 min at 20 min, 40 min, and 60 min after incubation started.

and connecting the **F** strand with **B** (**B-F** strand), opening and closing the tweezers is also possible [78]. Such integrated DNA machines equipped with photoresponsive DNA as the `engine` allows mechanical motion at very low concentrations, because the hybridization-dehybridization reaction (opening and closing) occurs not *intermoleclularly* but *intramolecularly*. By equipping photoresponsive DNA with a reversed switch, the photoswitching mode of the machine can be reversed [78]. Photoregulated DNA tweezers are one example that demonstrates the potential of photoresponsive DNA. Most DNA-fueled nanomachines can be easily converted to photon-fueled machines just by changing the fuel strand to a photoresponsive DNA. In this way, a variety of photon-fueled DNA-based nanomachines will be designed.

4.6. Photoregulation of Transcription with a Photoresponsive Promoter

Photoregulation of DNA hybridization depicted in Fig. (**6**) is certainly effective for a variety of applications related to DNA or RNA as described above. However, there is another strategy for the photoregulation of enzymatic reactions with "wedge-type" insertions of azobenzene. Far below the T_m, dissociation of the duplex does not occur even in the *cis*-form, but the local structure of the duplex around azobenzene changes by *trans-cis* isomerization, which affects interactions between DNA and enzymes. Under this condition, photoregulation of the binding and release of the enzyme to the azobenzene-tethered DNA is expected. RNA polymerase (RNAP) fits this strategy because it binds to sequence-specific promoter regions. The introduction of azobenzene on D-threoninol into the promoter region would allow photoregulation of transcription based on the change of local structure of the DNA duplex around the azobenzenes by *trans-cis* isomerization as schematically illustrated in Fig. (**13a**) [79], and not on the basis of photoregulation of hybridization as shown in Fig. (**6**).

T7 RNAP has been used because it is conventionally applied as a useful tool in biotechnology, and *in vitro* transla-

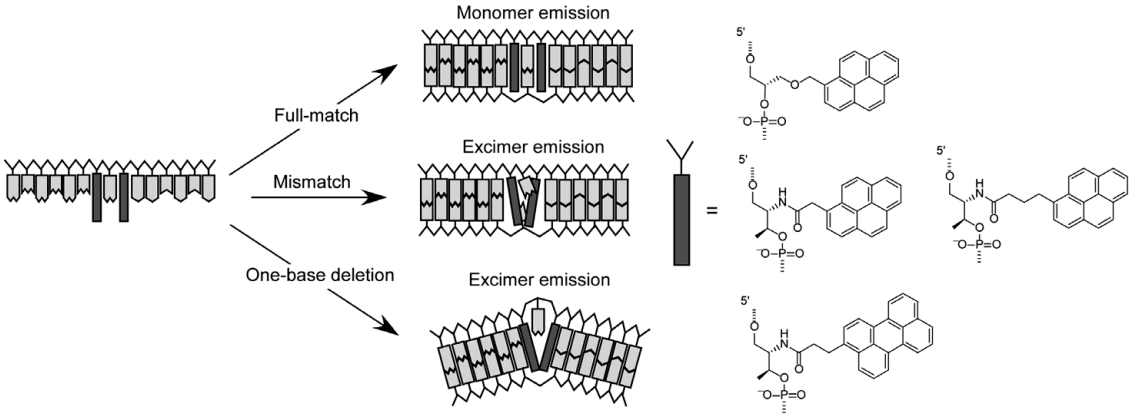

Fig. (14). Schematic illustration of the strategy for the detection of SNPs and/or indels based on the wedge-type insertion.

tion systems coupled with transcription have already been established for protein synthesis. The T7 promoter consists of two functional regions: an RNAP recognition region (from –11 to –4 nucleotides) where the loop of RNAP binds, and an unwinding region (from –4 to –1) that melts by the binding of RNAP (Fig. **13a**) [80]. Although photoregulation of transcription is possible with a photoresponsive promoter involving a single azobenzene at either the loop binding or unwinding region [79,81], the photoregulatory efficiency is insufficient. However, the simultaneous introduction of two azobenzenes into regions allows clear-cut photoregulation of transcription. For example, **N-9-3/T-Nt**, involving two azobenzenes in the non-template strand, interferes with transcription strongly under dark conditions. However, transcription is significantly accelerated after UV irradiation, resulting in high photoregulatory efficiency (about 8-fold acceleration). The synergistic effect of two azobenzenes for efficient photoregulation is conclusive. It should be noted that the *cis*-form maintains reasonably high transcription activity despite the introduction of two azobenzenes on D-threoninol. Since this photoswitching of transcription is totally reversible, repeated on-off switching by photo-irradiation is possible as depicted in Fig. (**13b**): UV irradiation turns on the photoswitch and visible light irradiation turns it off [58] Not only T7-RNAP, but also SP6-RNAP can be efficiently photoregulated by introducing two azobenzenes simultaneously at the loop binding and unwinding regions [82], suggesting that this strategy is applicable to other RNA polymerases and/or DNA-binding proteins.

5. FLUORESCENT DNA PROBES FOR DETECTING SNPS AND INDELS

Wedge-type insertions are also applicable to the sequence-specific recognition of DNA, such as the detection of single nucleotide polymorphisms (SNPs) and insertion/deletion (indel) polymorphisms. In the human genome, there are more than 300,000 known genetic polymorphisms, and the relationship between these differences and genetic diseases is under investigation [83]. To facilitate tailor-made medicine, various kinds of fluorescent probes have been proposed to detect genetic polymorphisms for high throughput analysis [84]. The basic strategy for the detection of SNPs and/or indels based on wedge-type insertions is schematically illustrated in Fig. (**14**) with pyrene and/or perylene that exhibits excimer emission [85-88]. Two dye moieties are tethered to DNA on both sides of the nucleotide for which we want to detect a SNP or deletion. When a fully-matched DNA hybridizes, both dye moieties intercalate and thus the interaction between the two dyes is suppressed by the intervening base-pair. As a result, only monomer emission is observed from the duplex ("full-match" in Fig. **15**). On the other hand, hybridization of this probe DNA with a mismatch, causing disordering around the mismatched base-pair, allows interaction of the two adjacent dyes that suppress (quench) monomer emission and exhibit excimer emission ("mismatch" in Fig. **15**). This effect is more evident for one-base deletion; the hybridization of the probe DNA with a deletion mutant results in a three-base bulge (including two pyrene moieties) being formed ("one-base deletion" in Fig. **14**). Here, two pyrene moieties are close enough to exhibit excimer emission. Thus, mismatch or deletion mutants can

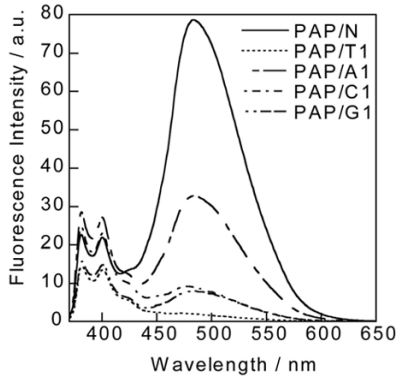

Fig. (15). Fluorescent emission spectra of **PAP/N** (one-base deletion mutant), **PAP/T1** (full-match), **PAP/A1** (mismatch), **PAP/C1** (mismatch), and **PAP/G1** (mismatch) at 0 ˚C. 1-Pyreneacetic acid is tethered on D-threoninol (**P** residue in the following sequence).
PAP:5'-GGTATC**P**A**P**GCAATC-3'
N:3'-CCATAGCGTTAG-5'
T1:3'-CCATAGTCGTTAG-5'
A1:3'-CCATAGACGTTAG-5'
C1:3'-CCATAGCCGTTAG-5'
G1:3'-CCATAGGCGTTAG-5'
Conditions: [NaCl] = 100 mM, pH 7.0 (10 mM phosphate buffer), [DNA] = 5 μM.
Excitation wavelength was 345 nm.

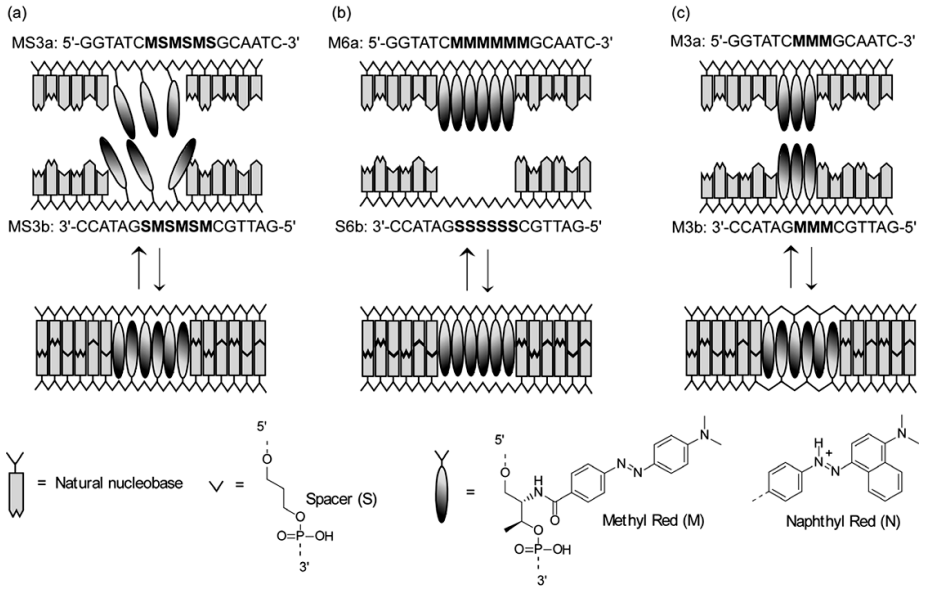

Fig. (16). Design for clustering of Methyl Reds with DNA conjugates. (**a**) Anti-parallel homo-cluster from **M**-**S** alternating sequence. (**b**) Parallel homo-cluster from consecutive **M** and **S** residues (c) Anti-parallel homo-cluster from consecutive **M** residues only.

be distinguished from fully-matched DNA by monitoring excimer emission. Both C2 (glycerol) [85] and C3 (threoninol) [86-88] scaffolds are available for this purpose.

Fig. (**15**) shows the fluorescent behavior of a pyrene probe tethered on a D-threoninol scaffold. When the fully-matched DNA **T1** is hybridized with a **PAP** probe involving two pyrenes on both sides of an intervening adenosine, only monomer emission (at around 380 and 400 nm) was observed (dotted line in Fig. **15**), demonstrating that two pyrene moieties intercalate and are detached from neighboring base-pairs. In contrast, hybridization with mismatched DNA (**A1, C1,** and **G1** in Fig. **15**) generates excimer emission at around 480 nm. The deletion mutant has a much stronger excimer emission. The hybridization of **PAP** with **N** that lacks thymidine (deletion mutant of **T1**) results in very strong excimer emission (solid line in Fig. **15**). The intensity of **PAP**/**N** at 500 nm is about 45-fold higher than that of **PAP**/**T1**. All these results demonstrate that two pyrenes are located in close proximity around the mismatched pair or in the bulge structure. Thus, mismatches and one-base deletions are easily distinguished from a fully-match DNA by monitoring the strength of excimer emission. Especially for the detection of base deletions, the advantage of this method is that we can design a probe that detects the deletion of two or even more bases by the use of 1-pyrenebutyric acid as well as 1-pyreneacetic acid (see the middle of Fig. **14**).

In addition to pyrene, perylene is also available for this purpose because it also exhibits excimer emission [89]. The advantages of perylene against pyrene are 1) its relatively high quantum yield, and 2) fluorescence in the visible region (ca. 460 and 490 nm) [90]. Hence, the use of perylene significantly improves sensitivity. In fact, a one-base deletion can be detected even at a lower concentration (the deletion mutant is distinguishable even at 5 nM) due to its high quantum yield. Furthermore, such differences can be detected even with the naked eye because both monomer and excimer emissions appear in the visible region [88]. Not only the excimer, but also an exciplex emission, such as a pyrene and *N*,*N*-dimethylaniline combination, is available for this strategy [87]. Recently, perylene bisimide on a C2 scaffold was applied to detect SNPs and indels [91]. Although the researchers did not adopt a wedge type insertion but instead replaced the natural nucleoside, polymorphisms were efficiently detected. These reports demonstrate the high potential of acyclic C2 and C3 scaffolds for sequence-specific recognition of DNA.

6. CLUSTERING OF NON-NATURAL MOLECULES ON THREONINOLS AS BASE-SURROGATES

Another application of the acyclic scaffold is the preparation of supramolecular arrays. As described in section **4.5**, DNA is also regarded as a nano-sized functional material as well as a carrier of genetic information [92]. The introduction of non-natural functional molecules diversifies the possible nano-architectures and functions. For example, metal arrays in DNA are prepared by introducing metal ligands consecutively into the base positions [93]. Arrays of fluorescence dyes are also created by consecutively introducing dyes into a single strand [94]. A zipper-like DNA motif that tethers aromatic non-natural bases on D-ribose stabilizes the duplex by interstrand stacking of the incorporated molecules [95]. In these cases, metal ligands or dyes are introduced at the C1′ position of D-ribose as non-natural bases. However, there is no limitation on the structure of a scaffold when DNAs are designed as supramolecular materials and are not enzymatically, but instead chemically synthesized. Non-natural scaffolds allow a variety of supramolecular structures that cannot be constructed with conventional D-ribose [96,97].

6.1. Design of Three Types of Homo-Cluster (H-aggregates) in the Duplex

By sequence design, three types of homo-clusters can be prepared as shown in Fig. (**16**). Here, Methyl Red is used as

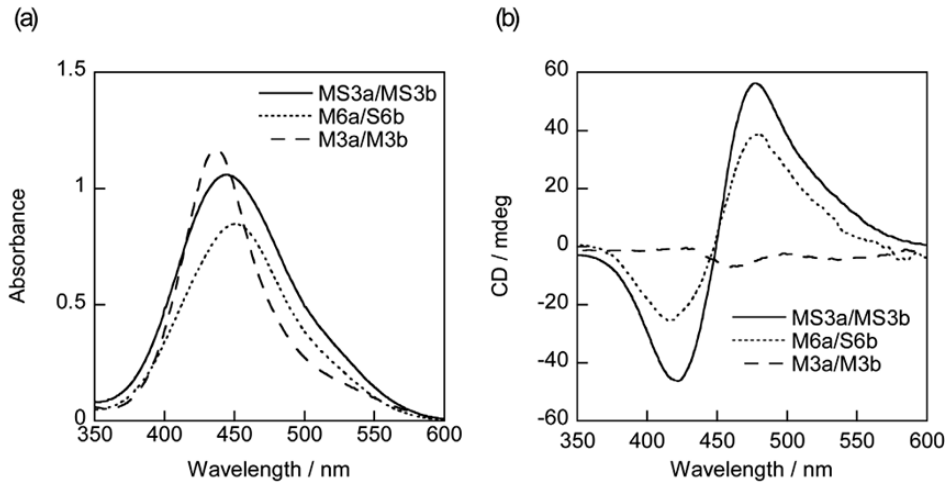

Fig. (17). UV-Vis (a) and CD spectra (b) of **MS3a/MS3b**, **M6a/S6b**, **M3a/M3b**
Conditions: [NaCl] = 100 mM, pH 7.0 (10 mM phosphate buffer), [DNA] = 5 μM.

a model dye because 1) the size of the dye fits the base pair, and 2) the asymmetric structure is suitable for demonstrating the effect of the relative orientation (parallel or anti-parallel) of the dye on the optical property, and 3) it has a single and fairly symmetrical absorption band. The first design is the anti-parallel clustering of Methyl Reds as depicted in Fig. (**16a**): Methyl Red on D-threoninol (**M** residues in Fig. **16**) and 1,3-propanediol (**S** in Fig. **16**) are alternately introduced at the center of the sequence [98, 99]. Here, the **S** residue is located at the counterpart of the **M** residue as a tentative "base-pair". At each side of the strand, natural nucleotides are attached as tags. With the aid of these natural nucleotides, two strands are hybridized and thus the dyes are forced to assemble at the center in the double-stranded DNA (**MS3a/MS3b** duplex in Fig. **16a**). By this design, dyes in the single-strand are almost isolated in the monomeric state whereas hybridization allows ordered clustering. NMR analysis directly demonstrates the homo-clustering (dimerization) of Methyl Reds, showing that two Methyl Reds are stacked anti-parallel to each other along the helix axis [100]. The clustering of Methyl Red by hybridization induces a hypsochromic shift that is characteristic of H-aggregation of dyes in which the dyes are stacked perpendicularly [101-103]. Concurrently, a positive couplet is strongly induced due to the right-handed helical structure by nature of D-threoninol that prefers clockwise winding. Accordingly, the use of L-threoninol induces much weaker CD due to the conflict of its counterclockwise winding with the clockwise winding of natural base-pairs on D-ribose [100].

The second design is a homo-parallel cluster of Methyl Reds, which is easily designed by the consecutive introduction of **M** residues as illustrated in Fig. (**16b**) [104]. Unlike the above anti-parallel cluster **MS3a**/**MS3b**, Methyl Reds are oriented in the same direction, namely they are stacked parallel in the single-stranded **M6a** because they are not separated by the **S** residues. Since Methyl Reds are close enough to be coupled excitonically in the single strand, a large hypsochromic shift is induced even in the single-stranded state. Hybridization of **M6a** with **S6b** involving six consecutive **S** residues counterpart to the **M** residues allows a Methyl Red homo-cluster in a parallel orientation in the duplex. On the basis of the change in the UV-Vis spectrum and CD, it appears that Methyl Reds form a parallel-assembled right-handed helix (*vide infra*) [104].

The third homo-cluster design does not require **S** residues as illustrated in Fig. (**16b**) and (**16c**) [105]. **M** residues are consecutively located at the counterpart of each strand to form a pseudo "base-pair" with an anti-parallel orientation. This **M**-**M** combination never interferes with duplex formation (clustering of Methyl Reds) but rather correlates with it. The T_m of the **M3a/M3b** duplex is 58.0 °C whereas that of the native duplex without **M** residues is 47.7 °C. The rate of T_m increase was 3.6 – 3.7 °C per **M**-**M** pair [105].

6.2. Comparison of Three Types of Dye Clusters in the Duplex

With **M** and **S** residues, three types of dye clusters are designed in the duplex: **MS3a/MS3b**, **M6a/S6b**, **M3a/M3b**, all of which involve six Methyl Reds (Fig. **16**). UV-Vis and CD spectra of all these clusters are depicted in Fig. (**17**). As this figure shows, **MS3a/MS3b** and **M6a/S6b**, both of which involve six **M** and six **S** residues, exhibit similar spectra. Absorption maxima of **MS3a/MS3b** and **M6a/S6b** are 444 and 448 nm, respectively, and the ICD intensities of both clusters are similar, demonstrating that right-handed winding structures were almost the same as illustrated in Fig. (**18a**) and (**18b**), except for the mutual orientation of the dyes: an anti-parallel stacked structure for **MS3a/MS3b** and a parallel stacked structure for **M6a/S6b**.

In the case of **M3a/M3b**, in which dyes are stacked anti-parallel as in **MS3a/MS3b**, the spectroscopic behavior is entirely different from the other two clusters: the UV-Vis spectrum shows larger hypsochromicity with a much narrower absorption band, and ICD is far smaller, being interpreted as a firmly stacked unwound structure as depicted in Fig. (**18c**). Methyl Reds in **MS3a/MS3b** (Fig. **18a**) form a right-handed helix resembling natural B-type DNA, and the removal of an **S** residue (**M3a/M3b**) makes the helix rewind. In **MS3a/MS3b**, winding makes the Methyl Reds stack because an **S** residue separates each **M** residue. But in the ab-

Fig. (18). Illustration of the structure of **MS3a/MS3b**, **M6a/S6b** and **M3a/M3b** estimated from UV-Vis and CD spectra shown in Fig. (**17**).

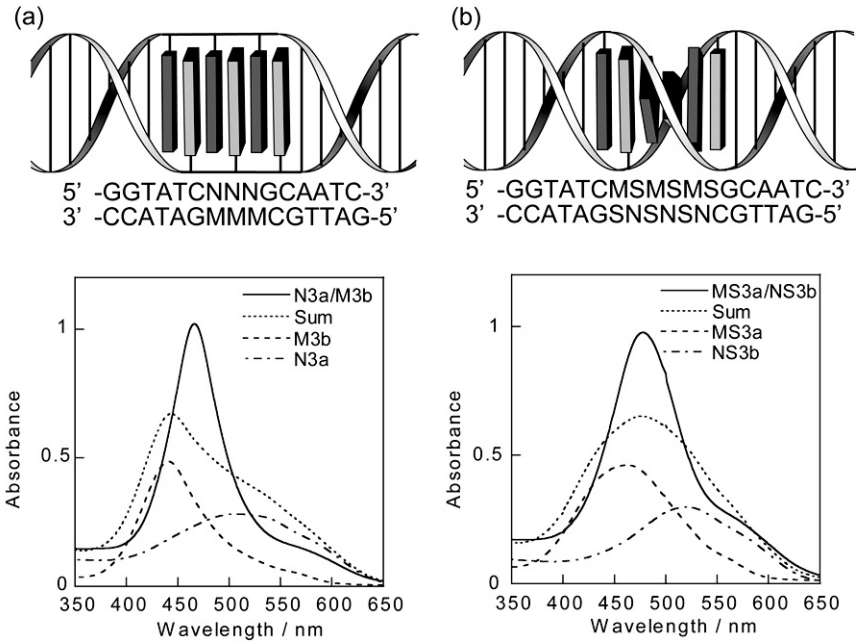

Fig. (19). Schematic illustration (upper panel) of the hetero aggregates and their UV-Vis spectra (lower panel) of (**a**) **N3a**/**M3b** and (**b**) **MS3a**/**NS3b** monitored at 0 ^{o}C. See Fig. (**16**) for the structure of Naphthyl Red (**N**).
Conditions: [NaCl] = 100 mM, pH 5.0 (10 mM MES buffer), [DNA] = 5 μM.

sence of **S**, Methyl Reds do not need winding in order to form a firmly stacked structure. In addition, the threoninol scaffold allows such a ladder-like structures due to its flexibility.

6.3. Hetero-Clustering of the Dyes

By use of threoninol-tethered dyes, various aggregates that have been impossible to prepare by the conventional self-association of dyes are easily programmable. Alternating hetero-clusters [106], in which two different dyes are stacked alternately, is one example. Such alternating hetero-clusters can easily be prepared by hybridizing two complementary DNA-dye conjugates, each of which involves a different dye as illustrated in Fig. (**19a**) and (**19b**). Here, both Methyl Red (**M** residue) and Naphthyl Red (**N** residue) are tethered on D-threoninols for constructing hetero-clusters. Aqueous solutions of **N3a** and **M3b,** each of which tether three consecutive Naphthyl Reds or Methyl Reds, exhibit absorption maxima at 506 and 441 nm, as shown by broken and dotted broken lines in Fig. (**19a**), respectively. Interestingly, when these two strands hybridize, a new single sharp band appears at 466 nm (solid line in Fig. **19**). A simple sum of the spectra of single-stranded **N3a** and **M3b** (dotted lines in Fig. **19a**) is entirely different from the spectrum of the **N3a/M3b** duplex (compare solid with dotted line in Fig. **19a**) [105]. Similarly, the **MS3a/NS3b** duplex involving an **S** residue between the **M** or **N** residues exhibits a similar merging of the two bands as depicted in Fig. (**19b**) [107]. These spectroscopic behaviors demonstrate that Methyl Red and Naphthyl Red in the hetero aggregates optically interact each other (H-band) and provide different spectroscopic properties from those in the monomeric states. This might be one of the few successful H-aggregates containing two different kinds of dyes exhibiting a single sharp band. By use of DNA conjugates, hetero-clusters can be easily prepared just by mixing two complementary strands.

7. CONCLUSION

In the present review, we focused on the modification of DNA by the use of acyclic scaffolds, particularly with regard to our recent works using threoninol. Various functional DNAs have been prepared with this scaffold by wedge-type insertion into DNA or tentative "base-pairing" of dyes on threoninols for clustering without destabilizing the duplex. Not only C3, but also C2 scaffolds based on glycerol or 3-amino-1,2-propanediol are available for these purposes

[108]. Furthermore, these acyclic scaffolds can be used to tether cationic molecules that are hard to incorporate into the C1' position of D-ribose due to decomposition during DNA synthesis on an automated synthesizer and the deprotection process thereafter [109,110]. Several applications have been realized, such as photoregulation of DNA functions, development of fluorescence probes for detecting SNPs and indels, and construction of dye clusters. We believe that these advantages are promising for diverse application of acyclic linkers to construct a variety of artificial DNAs used in molecular computers, conductive nano-wires, nano-machines, effective antisense DNA (or siRNA), or artificially controlled genes involving photoswitches, which will be produced in the near future.

ACKNOWLEDGEMENTS

This work was supported by the Core Research for Evolution Science and Technology (CREST), Japan Science and Technology Agency (JST). Part of this work was also supported by a Grant-in-Aid for Specially Promoted Scientific Research from the Ministry of Education, Culture, Sports, Science and Technology, Japan, and The Mitsubishi Foundation (to H.A.). We also express special thanks to Professor Makoto Komiyama (RCAST, The Univ. of Tokyo) for his very useful advice and comments.

REFERENCES

[1] Sakamoto, K.; Gouzu, H.; Koyama, K.; Kiga, D.; Yokoyama, S.; Yokomori, T.; Hagiya, M. Molecular computation by DNA hairpin formation. *Science*, **2000**, *288*, 1223-1226.

[2] Murphy, C.J.; Arkin, M.R.; Jenkins, Y.; Ghatlia, N.D.; Bossmann, S.H.; Turro, N.J.; Barton, J.K. Long-range photoinduced electron transfer through a DNA helix. *Science*, **1993**, *262*, 1025-1029.

[3] Simmel, F. C.; Yurke, B. Using DNA to construct and power a nanoactuator. *Phys. Rev. E*, **2001**, *63*, 041913.

[4] Rothemund, P.W.K. Folding DNA to create nanoscale shapes and patterns. *Nature*, **2006**, *440*, 297-302.

[5] Virta, P.; Katajisto, J.; Niittymäki, T.; Lönnberg, H. Solid-supported synthesis of oligomeric bioconjugates. *Tetrahedron*, **2003**, *59*, 5137-5174.

[6] French, D.J.; Archard, C.L.; Brown, T.; McDowell, D.G. HyBeacon (TM) probes: a new tool for DNA sequence detection and allele discrimination. *Mol. Cell. Probes*, **2001**, *15*, 363-374.

[7] Hwang, G.T.; Seo, Y.J.; Kim, B.H. A highly discriminating quencher-free molecular beacon for probing DNA. *J. Am. Chem. Soc*., **2004**, *126*, 6528-6529.

[8] Yamana, K.; Aota, R.; Nakano, H. Oligonucleotides having covalently linked anthracene at specific sugar residue: Differential binding to DNA and RNA and fluorescence properties. *Tetrahedron Lett.*, **1995**, *36*, 8427-8430.

[9] Yamana, K.; Zako, H.; Asazuma, K.; Iwase, R.; Nakano, H.; Murakami, A. Fluorescence detection of specific RNA sequences using 2'-pyrene-modified oligoribonucleotides. *Angew. Chem. Int. Ed*., **2001**, *40*, 1104-1106.

[10] Letsinger R.L.; Schott, M.E. Selectivity in binding a phenanthridinium-dinucleotide derivative to homopolynucleotides. *J. Am. Chem. Soc*., **1981**, *103*, 7394-7396.

[11] Okamoto, A.; Kanatani, K.; Saito, I. Pyrene-labeled base-discriminating fluorescent DNA probes for homogeneous SNP typing. *J. Am. Chem. Soc*., **2004**, *126*, 4820-4827.

[12] Mahara, A.; Iwase, R.; Sakamoto, T.; Yamana, K.; Yamaoka, T.; Murakami, A. Bispyrene-conjugated 2 '-O-methyloligonucleotide as a highly specific RNA-recognition probe. *Angew. Chem. Int. Ed*., **2002**, *41*, 3648-3650.

[13] Hocek, M.; Fojta, M. Cross-coupling reactions of nucleoside triphosphates followed by polymerase incorporation. Construction and applications of base-functionalized nucleic acids. *Org. Biomol. Chem.*, **2008**, *6*, 2233-2241.

[14] Oka, N.; Wada, T.; Saigo, K. An oxazaphospholidine approach for the stereocontrolled synthesis of oligonucleoside phosphorothioates. *J. Am. Chem. Soc*., **2003**, *125*, 8307-8317.

[15] Zatsepin, T.S.; Gait, M.J.; Oretskaya, T.S. 2 '-functionalized nucleic acids as structural tools in molecular biology. *IUBMB Life*, **2004**, *56*, 209-214.

[16] Usman, N.; Juby, C.D.; Ogilvie, K.K. Preparation of glyceronucleoside phosphoramidite synthons and their use in the solid phase synthesis of acyclic oligonucleotides. *Tetrahedron Lett.*, **1988**, *29*, 4831-4834.

[17] Nelson, P.S.; Kent, M.; Muthini, S. Oligonucleotide labeling methods 3. Direct labeling of oligonucleotides employing a novel, non-nucleosidic, 2-aminobutyl-1,3-propanediol backbone. *Nucleic Acids Res.*, **1992**, *20*, 6253-6259.

[18] Vandendriessche, F.; Augustyns, K.; Aerschot, A.V.; Busson, R.; Hoogmartens, J.; Herdewijn, P. Acyclic oligonucleotides: possibilities and limitations. *Tetrahedron*, **1993**, *49*, 7223-7238.

[19] Nielsen, P.; Kirpekar, F.; Wengel, J. Incorporation of (R)- and (S)-3',4'-seco-thymidine into oligodeoxynucleotides: hybridization properties and enzymatic stability. *Nucleic Acids Res.*, **1994**, *22*, 703-710.

[20] Endo, M.; Saga, Y.; Komiyama, M. A novel phosphoramidite for the site-selective introduction of functional groups into oligonucleotides via versatile tethers. *Tetrahedron Lett.*, **1994**, *35*, 5879-5882.

[21] Fino, J.R.; Mattingly, P.G.; Ray, K.A. A Convenient Method for the Preparation of Hapten Phosphoramidites. *Bioconjug. Chem.*, **1996**, *7*, 274-280.

[22] Ramasamy K.S.; Seifert, W. Amino acid nucleic acids: synthesis and hybridization properties of a novel class of antisense oligonucleotides. *Bioorg. Med. Chem. Lett.*, **1996**, *6*, 1799-1804.

[23] Rana, V.S.; Kumar, V.A.; Ganesh, K.N. Oligonucleotides with (N-thymin-1-ylacetyl) 1-phenylserinol in backbone: Chiral acyclic analogues that form dna triplexes. *Bioorg. Med. Chem. Lett.*, **1997**, *7*, 2837-2842.

[24] Yamana, K.; Takei, M.; Nakano, H. Synthesis of oligonucleotide derivatives containing pyrene labeled glycerol linkers: Enhhanced excimer fluorescence on binding to a complementary DNA sequence. *Tetrahedron Lett.*, **1997**, *38*, 6051-6054.

[25] Xiang, G.; McLaughlin, L.W. A cytosine analogue containing a conformationally flexible acyclic linker for triplex formation at sites with contiguous G-C base pairs. *Tetrahedron*, **1998**, *54*, 375-392.

[26] Trawick, B.N.; Osiek, T.A.; Bashkin, J.K. Enhancing Sequence-Specific Cleavage of RNA within a Duplex Region: Incorporation of 1,3-Propanediol Linkers into Oligonucleotide Conjugates of Serinol-Terpyridine. *Bioconjug. Chem.*, **2001**, *12*, 900-905.

[27] Ueno, Y.; Mikawa, M.; Hoshino, S.; Matsuda, A. Nucleosides and Nucleotides. 208. Alternate-Strand Triple-Helix Formation by the 3'-3'-Linked Oligodeoxynucleotides with the Anthraquinonyl Group at the Junction Point. *Bioconjug. Chem.*, **2001**, *12*, 635-642.

[28] Dioubankova, N.N.; Malakhov, A.D.; Stetsenko, D.A.; Korshun, V.A.; Gait, M.J. (R)-2,4-Dihydroxybutyramide seco-Pseudonucleosides: New Versatile Homochiral Synthons for Synthesis of Modified Oligonucleotides. *Org. Lett.*, **2002**, *4*, 4607-4610.

[29] Yamana, K.; Iwai, T.; Ohtani, Y.; Sato, S.; Nakamura, M.; Nakano, H. Bis-Pyrene-Labeled Oligonucleotides: Sequence Specificity of Excimer and Monomer Fluorescence Changes upon Hybridization with DNA. *Bioconjug. Chem.*, **2002**, *13*, 1266-1273.

[30] Christensen, U.B., Pedersen, E.B. Intercalating nucleic acids containing insertions of 1-O-(1-pyrenylmethyl)glycerol: stabilisation of dsDNA and discrimination of DNA over RNA. *Nucleic Acids Res.*, **2002**, *30*, 4918-4925.

[31] Petersen, A.B.; Petersen, M.Å.; Henriksen, U.; Hammerum, S.; Dahl, O. Acyclic, achiral enamide nucleoside analogues. The importance of the C=C bond in the analogue for its ability to mimic natural nucleosides. *Org. Biomol. Chem.*, **2003**, *1*, 3293-3296.

[32] Huber, R.; Amann, N.; Wagenknecht, H.-A. Synthesis of DNA with Phenanthridinium as an Artificial DNA Base. *J. Org. Chem.*, **2004**, *69*, 744-751.

[33] Okamoto, A.; Ichiba, T.; Saito, I. Pyrene-labeled oligodeoxynucleotide probe for detecting base insertion by excimer fluorescence emission. *J. Am. Chem. Soc*., **2004**, *126*, 8364-8365.

[34] Ueno, Y.; Ishihara, S.; Ito, Y.; Kitade, Y. Synthesis of 2 ',5 '-oligoadenylate analogs containing an adenine acyclonucleoside and

their ability to activate human RNase L. *Bioorg. Med. Chem. Lett.*, **2004**, *14*, 4431-4434.

[35] Zhang, L.; Meggers, E. An Extremely Stable and Orthogonal DNA Base Pair with a Simplified Three-Carbon Backbone. *J. Am. Chem. Soc*., **2005**, *127*, 74-75.

[36] Reynolds, M.A.; Beck, T.A.; Hogrefe, R.I.; McCaffrey, A.; Arnold, L.J.Jr; Vaghefi, M.M. A non-nucleotide-based linking method for the preparation of psoralen-derivatized methylphosphonate oligonucleotides. *Bioconjug. Chem*., **1992**, *3*, 366-374.

[37] Fukui, K.; Morimoto, M.; Segawa, H.; Tanaka, K.; Shimidzu, T. Synthesis and Properties of an Oligonucleotide Modified with an Acridine Derivative at the Artificial Abasic Site. *Bioconjug. Chem*., **1996**, *7*, 349-355.

[38] Fukui, K.; Iwane, K.; Shimidzu, T.; Tanaka, K. Oligonucleotides covalently linked to an acridine at artificial abasic site: Influence of linker length and the base-sequence. *Tetrahedron Lett*., **1996**, *37*, 4983-4986.

[39] Asanuma, H.; Takarada, T.; Yoshida, T.; Tamaru, D.; Liang, X.G.; Komiyama, M. Enantioselective incorporation of azobenzenes into oligodeoxyribonucleotide for effective. photoregulation of duplex formation *Angew. Chem. Int. Ed.*, **2001**, *40*, 2671-2673.

[40] Liang, X.G.; Asanuma, H.; Kashida, H.; Takasu, A.; Sakamoto, T.; Kawai, G.; Komiyama, M. MR study on the photoresponsive DNA tethering an azobenzene. Assignment of the absolute configuration of two diastereomers and structure determination of their duplexes in the *trans*-form. *J. Am. Chem. Soc*., **2003**, *125*, 16408-16415.

[41] Asanuma, H.; Ito, T.; Komiyama, M. Photo-responsive oligonucleotides carrying azobenzene in the side-chains. *Tetrahedron Lett*., **1998**, *39*, 9015-9018.

[42] Asanuma, H.; Ito, T.; Yoshida, T.; Liang, X.G.; Komiyama, M. Photoregulation of the formation and dissociation of a DNA duplex by using the cis-trans isomerization of azobenzene. *Angew. Chem. Int. Ed*., **1999**, *38*, 2393-2395.

[43] Arnott, S.; Dover, S.D.; Wonacott, A.J. Least-squares refinement of the crystal and molecular structures of DNA and RNA from X-ray data and standard bond lengths and angles. *Acta Crystallogr*., *Sect. B: Struct. Crystallogr. Cryst. Chem*., **1969**, *25*, 2192-2206.

[44] Brotschi, C.; Leumann, C. J. DNA with Hydrophobic Base Substitutes: A Stable, Zipperlike Recognition Motif Based On Interstrand-Stacking Interactions. *Angew. Chem. Int. Ed*., **2003**, *42*, 1655-1658.

[45] Tanaka, F.; Kameda, A.; Yamamoto, M.; Ohuchi, A. Thermodynamic Parameters Based on a Nearest-Neighbor Model for DNA Sequences with a Single-Bulge Loop. *Biochemistry*, **2004**, *43*, 7143-7150.

[46] Asanuma, H.; Matsunaga, D.; Komiyama, M. Clear-cut photoregulation of the formation and dissociation of the DNA duplex by modified oligonucleotide involving multiple azobenzenes. *Nucleic Acids Symp. Ser*., **2005,** *49*, 35-36.

[47] Asanuma, H.; Hayashi, H.; Zhao, J.; Liang, X.G.; Yamazawa, A.; Kuramochi, T.; Matsunaga, D.; Aiba, Y.; Kashida, H.; Komiyama, M. Enhancement of RNA cleavage activity of 10-23 DNAzyme by covalently introduced intercalator. *Chem. Commun*., **2006**, 5062-5064.

[48] Filichev, V.V.; Hilmy, K.M.H.; Christensen, U.B.; Pedersen, E.B. Intercalating nucleic acids: the inversion of the stereocentre in 1-O-(pyren-1-ylmethyl)glycerol from R to S. Thermal stability towards ssDNA, ssRNA and its own type of oligodeoxynucleotides. *Tetrahedron Lett*., **2004**, *45*, 4907-4910.

[49] Mayer, G.; Heckel, A. Biologically active molecules with a "light switch". *Angew. Chem. Int. Ed*., **2006**, *45*, 4900-4921.

[50] Willner, I.; Rubin, S. Control of the structure and functions of biomaterials by light. *Angew. Chem. Int. Ed*., **1996**, *35*, 367-385.

[51] Simons, M.; Kramer, E.M.; Thiele, C.; Stoffel, W.; Trotter, J. Assembly of myelin by association of proteolipid protein with cholesterol- and galactosylceramide-rich membrane domains. *J. Cell Biol.*, **2000**, *151*, 143-153.

[52] Mintzer, E.A.; Warrts, B.L.; Wilschut, J.; Bittman, R. Behavior of a photo activatable analog of cholesterol, 6-photocholesterol, in model membranes. *FEBS Lett.*, **2002**, *39*, 181-184.

[53] Rothman, D.M.; Shults, M.D.; Imperiali, B. Chemical approaches for investigating phosphorylation in signal transduction networks. *Trends Cell Biol*., **2005**, *15*, 502-510.

[54] Yamana, K.; Yoshikawa, A.; Nakao, N. Synthesis of a new photoisomerizable linker for connecting two oligonucleotide segments *Tetrahedron Lett.*, **1996**, *37*, 637-640.

[55] Liu, Y.; Sen, D. A contact photo-cross-linking investigation of the active site of the 8-17 deoxyribozyme. *J. Mol. Biol*., **2004**, *341*, 887-892.

[56] Keiper, S.; Vyle, J.S. Reversible photocontrol of deoxyribozyme-catalyzed RNA cleavage under multiple-turnover conditions. *Angew. Chem. Int. Ed*., **2006**, *45*, 3306-3309.

[57] Nishioka, H.; Liang, X.G.; Kashida, H.; Asanuma, H. 2 ',6 '-Dimethylazobenzene as an efficient and thermo-stable photoregulator for the photoregulation of DNA hybridization. *Chem. Commun*., **2007**, 4354-4356.

[58] Asanuma, H.; Liang, X.G.; Nishioka, H.; Matsunaga, D.; Liu, M.; Komiyama, M. Synthesis of azobenzene-tethered DNA for reversible photo-regulation of DNA functions: hybridization and transcription. *Nat. Protoc*., **2007**, *2*, 203-212.

[59] Asanuma, H.; Liang, X.G.; Yoshida, T.; Yamazawa, A.; Komiyama, M. Photocontrol of triple-helix formation by using azobenzene-bearing oligo(thymidine). *Angew. Chem. Int. Ed*., **2000**, *39*, 1316-1318.

[60] Liang, X.G.; Asanuma, H.; Komiyama, M. Photoregulation of DNA triplex formation by azobenzene. *J. Am. Chem. Soc*., **2002**, *124*, 1877-1883.

[61] Takarada, T.; Tamaru, D.; Liang, X.G.; Komiyama, M. L-threoninol as a chiral linker of azobenzene for the effective photoregulation of DNA tripler formation. *Chem. Lett*., **2001**, 732-733.

[62] Liang, X.G.; Asanuma, H.; Komiyama, M. Phenylazonaphthalene as a superb photo-regulator for DNA-triplex formation. *Tetrahedron Lett*., **2001**, *42*, 6723-6725.

[63] Filichev, V.V.; Pedersen, E.B. Stable and selective formation of Hoogsteen-type triplexes and duplexes using twisted intercalating nucleic acids (TINA) prepared via postsynthetic sonogashira solid-phase coupling reactions. *J. Am. Chem. Soc*., **2005**, *127*, 14849-14858.

[64] Barre, F.X.; Giovannangeli, C.; Hélène, C.; Harel-Bellan, A. Covalent crosslinks introduced via a triple helix-forming oligonucleotide coupled to psoralen are inefficiently repaired. *Nucleic Acids Res.*, **1999**, *27*, 743-749.

[65] Liang, X.G.; Takenaka, N.; Nishioka, H.; Asanuma, H. Molecular design for reversing the photoswitching mode of turning ON and OFF DNA hybridization. *Chem. Asian J*., **2008**, *3*, 553-560.

[66] Yamazawa, A.; Liang, X.G.; Asanuma, H.; Komiyama, M. Photoregulation of the DNA polymerase reaction by oligonucleotides bearing an azobenzene. *Angew. Chem. Int. Ed*., **2000**, *39*, 2356-2357.

[67] Matsunaga, D.; Asanuma, H.; Komiyama, M. Photoregulation of RNA digestion by RNase H with azobenzene-tethered DNA. *J. Am. Chem. Soc*., **2004**, *126*, 11452-11453.

[68] Chiang, M.Y.; Chan, H.; Zounes, M.A.; Freier, S.M.; Lima, W.F.; Bennett, C.F. Antisense oligonucleotides inhibit intercellular adhesion molecule 1 expression by two distinct mechanisms. *J. Biol. Chem*., **1991**, *266*, 18162-18171.

[69] Chen, J.; Seeman, N.C. Synthesis from DNA of a molecule with the connectivity of a cube. *Nature*, **1991**, *350*, 631-633.

[70] Beissenhirtz, M.K.; Willner, I. DNA-based machines. *Org. Biomol. Chem.*, **2006**, *4*, 3392-3401.

[71] Seeman, N. C.; Lukeman, P. S. Nucleic acid nanostructures: bottom-up control of geometry on the nanoscale. *Rep. Prog. Phys*., **2005**, *68*, 237-270.

[72] Shih, W.M.; Quispe, J.D.; Joyce, G.F. A 1.7-kilobase single-stranded DNA that folds into a nanoscale octahedron. *Nature*, **2004**, *427*, 618-621.

[73] Shin, J. S.; Pierce, N. A. A synthetic DNA walker for molecular transport. *J. Am. Chem. Soc.*, **2004**, *126*, 10834-10835.

[74] Tian, Y.; Mao, C. D. Molecular gears: A pair of DNA circles continuously rolls against each other. *J. Am. Chem. Soc.*, **2004**, *126*, 11410-11411.

[75] Beyer, S.; Simmel, F. C. A modular DNA signal translator for the controlled release of a protein by an aptamer. *Nucleic Acid Res.*, **2006**, *34*, 1581-1587.

[76] Yurke, B.; Turberfield, A.J.; Mills, A.P. Jr; Simmel, F.C.; Neumann, J.L. A DNA-fuelled molecular machine made of DNA. *Nature*, **2000**, *406*, 605-608.

[77] Liang, X.G.; Nishioka, H.; Takenaka, N.; Asanuma, H. A DNA nanomachine powered by light irradiation. *ChemBioChem*, **2008**, *9*, 702-705.

[78] Liang, X.G.; Takenaka, N.; Nishioka, H.; Asanuma, H. Light driven open/close operation of an azobenzene-modified DNA

nano-pincette. *Nucleic Acids Symp. Ser*., **2008**, *52*, 697-698.
[79] Liu, M.; Asanuma, H.; Komiyama, M. Azobenzene-tethered T7 promoter for efficient photoregulation of transcription. *J. Am. Chem. Soc*., **2006**, *128*, 1009-1015.
[80] Cheetham, G.M.T.; Jeruzalmi, D.;Steitz, T.A. Structural basis for initiation of transcription from an RNA polymerase-promoter complex. *Nature*, **1999**, *399*, 80-83.
[81] Asanuma, H.; Tamaru, D.; Yamazawa, A.; Liu, M.; Komiyama, M. Photoregulation of the transcription reaction of T7 RNA polymerase by tethering an azobenzene to the promoter. *ChemBioChem*, **2002**, *3*, 786-789.
[82] Liu, M.; Tamaru, D.; Asanuma, H.; Komiyama, M. Synergistic effect of the two azobenzenes in the promoter on the photoregulation of transcription reaction with SP6 RNA polymerase. *Chem. Lett*., **2003**, *32*, 1174-1175.
[83] Tsongalis, G. J.; Coleman, W. B. Clinical genotyping: The need for interrogation of single nucleotide polymorphisms and mutations in the clinical laboratory. *Clin. Chim. Acta*, **2006**, *363*, 127-137.
[84] Kool, E. T. Replacing the nucleohases in DNA with designer molecules. *Acc. Chem. Res*., **2002**, *35*, 936-943.
[85] Christensen U. B.; Pedersen, E. B. Intercalating Nucleic Acids with Pyrene Nucleotide Analogues as Next-Nearest Neighbors for Excimer Fluorescence Detection of Single-Point Mutations under Nonstringent Hybridization Conditions. *Helv. Chim. Acta*, **2003**, *86*, 2090-2097.
[86] Kashida, H.; Asanuma, H.; Komiyama, M. Insertion of two pyrene moieties into oligodeoxyribonucleotides for the efficient detection of deletion polymorphisms. *Chem. Commun*., **2006**, 2768-2770.
[87] Kashida, H.; Komiyama, M.; Asanuma, H. Exciplex formation between pyrene and N,N-dimethylaniline in DNA for the detection of one-base deletion. *Chem. Lett*., **2006**, *35*, 934-935.
[88] Kashida, H.; Takatsu, T.; Asanuma, H. Detection of genetic polymorphisms with high sensitivity by DNA-perylene conjugate. *Tetrahedron Lett*., **2007**, *48*, 6759-6762.
[89] Tanaka, J. The Electronic Spectra of Aromatic Molecular Crystals. II. The Crystal Structure and Spectra of Perylene. *Bull. Chem. Soc. Jpn*., **1963**, *36*, 1237-1249.
[90] Komfort, M.; Löhmannsröben, H.G.; Salthammer, T. The temperature dependence of photophysical processes in perylene, tetracene and some of their derivatives. *J. Photochem. Photobiol. A*, **1990**, *51*, 215-227.
[91] Baumstark, D.; Wagenknecht, H.-A. Perylene Bisimide Dimers as Fluorescent "Glue" for DNA and for Base-Mismatch Detection. *Angew. Chem. Int. Ed*., **2008**, *47*, 2612-2614.
[92] Seeman, N.C. An overview of structural DNA Nanotechnology *Mol. Biotechnol*., **2007**, *37*, 246-257.
[93] Tanaka, K.; Tengeiji, A.; Kato, T.; Toyama, N.; Shionoya, M. A discrete self-assembled metal array in artificial DNA. *Science*, **2003**, *299*, 1212-1213.
[94] Gao, J.; Strässler, C.; Tahmassebi, D.; Kool, E.T. Libraries of Composite Polyfluors Built from Fluorescent Deoxyribosides. *J. Am. Chem. Soc.*, **2002**, *124*, 11590-11591.
[95] Brotschi, C.; Mathis, G.; Leumann, C. J. Bipyridyl- and Biphenyl-DNA: A Recognition Motif Based on Interstrand Aromatic Stacking. *Chem. Eur. J.*, **2005**, *11*, 1911-1923.
[96] Langenegger, S. M.; Häner, R. The effect of a non-nucleosidic phenanthrene building block on DNA duplex stability. *Helv. Chim. Acta*, **2002**, *85*, 3414-3421.
[97] Samain, F.; Malinovskii, V. L.; Häner, R. Spectroscopic properties of pyrene-containing DNA mimics. *Bioorg. Med. Chem*., **2008**, *16*, 27-33.
[98] Asanuma, H.; Shirasuka, K.; Komiyama, M. H-aggregation of methyl reds by the hybridization of DNA-dye conjugates. *Chem. Lett*., **2002**, 490-491.
[99] Kashida, H.; Asanuma, H.; Komiyama, M. Interstrand H-aggregation of cationic dyes for narrowing the absorption spectra and stabilizing the duplex. *Supramol. Chem*., **2004**, *16*, 459-464.
[100] Kashida, H.; Tanaka, M.; Baba, S.; Sakamoto, T.; Kawai, G.; Asanuma, H.; Komiyama, M. Covalent incorporation of methyl red dyes into double-stranded DNA for their ordered clustering. *Chem. Eur. J*., **2006**, *12*, 777-784.
[101] McRae, E.G.; Kasha, M. Enhancement of Phosphorescence Ability upon Aggregation of Dye Molecules. *J. Chem. Phys*., **1958**, *28*, 721-722.
[102] Herz, A.H. Dyedye interactions of cyanines in solution and at AgBr surfaces. *Photogr. Sci. Eng*., **1974**, *18*, 323-335.
[103] Tanaka, J. *Relaxation of Elementary Excitations*, Kubo, R., Hanamura, F., Ed.; Springer Verlag: New York, **1980**, p. 181.
[104] Asanuma, H.; Shirasuka, K.; Takarada, T.; Kashida, H.; Komiyama, M. DNA-dye conjugates for controllable H* aggregation. *J. Am. Chem. Soc*., **2003**, *125*, 2217-2223.
[105] Kashida, H.; Fujii, T.; Asanuma, H. Threoninol as a scaffold of dyes (threoninol-nucleotide) and their stable interstrand clustering in duplexes. *Org. Biomol. Chem*., **2008**, *6*, 2892-2899.
[106] Makio, S.; Kanamaru, N.; Tanaka, J. The J-aggregate 5,5',6,6'-Tetrachloro-1,1'-diethyl-3,3'-bis(4-sulfobutylbenzimidazolocarbocyanine Sodium Salt in Aqueous Solution. *Bull. Chem. Soc. Jpn*., **1980**, *53*, 3120-3124.
[107] Kashida, H.; Asanuma, H.; Komiyama, M. Alternating hetero H aggregation of different dyes by interstrand stacking from two DNA-dye conjugates. *Angew. Chem. Int. Ed*., **2004**, *43*, 6522-6525.
[108] Baumstark, D.; Wagenknecht, H.-A. Fluorescent Hydrophobic Zippers inside Duplex DNA: Interstrand Stacking of Perylene-3,4:9,10-tetracarboxylic Acid Bisimides as Artificial DNA Base Dyes. *Chem. Eur. J*., **2008**, *14*, 6640-6645.
[109] Menacher, F.; Rubner, M.; Berndl, S.; Wagenknecht, H.-A. Thiazole Orange and Cy3: Improvement of Fluorescent DNA Probes with Use of Short Range Electron Transfer. *J. Org. Chem*., **2008**, *73*, 4263-4266.
[110] Asanuma, H.; Hara, Y.; Noguchi, A.; Sano, K.; Kashida, H. Post-synthetic modification of DNA via threoninol on a solid support by means of allylic protection. *Tetrahedron Lett*., **2008**, *49*, 5144-5146.